Wedge holography in flat space and celestial holography

Naoki Ogawa[1], Tadashi Takayanagi[1,2,3] Takashi Tsuda,[1] and Takahiro Waki[1]

[1]*Center for Gravitational Physics and Quantum Information, Yukawa Institute for Theoretical Physics, Kyoto University, Kitashirakawa Oiwakecho, Sakyo-ku, Kyoto 606-8502, Japan*
[2]*Inamori Research Institute for Science, 620 Suiginya-cho, Shimogyo-ku, Kyoto 600-8411 Japan*
[3]*Kavli Institute for the Physics and Mathematics of the Universe (WPI), University of Tokyo, Kashiwa, Chiba 277-8582, Japan*

In this paper, we study codimension two holography in flat spacetimes, based on the idea of the wedge holography. We propose that a region in a $d + 1$ dimensional flat spacetime surrounded by two end of the world branes, which are given by d dimensional hyperbolic spaces, is dual to a conformal field theory (CFT) on a $d - 1$ dimensional sphere. Similarly, we also propose that a $d + 1$ dimensional region in the flat spacetime bounded by two d dimensional de Sitter spaces is holographically dual to a CFT on a $d - 1$ dimensional sphere. Our calculations of the partition function, holographic entanglement entropy and two point functions, support these duality relations and imply that such CFTs are nonunitary. Finally, we glue these two dualities along null surfaces to realize a codimension two holography for a full Minkowski spacetime and discuss a possible connection to the celestial holography.

I. INTRODUCTION

The holographic principle [1,2] usually relates a gravitational theory on a certain spacetime M to a nongravitational theory on its codimension one boundary ∂M. This holographic property is manifest in the AdS/CFT [3] and the dS/CFT [4,5]. However, if we try to apply the usual analysis of bulk to boundary relation in the AdS/CFT [6,7] to a $d + 1$ dimensional flat Lorentzian spacetime, its mathematical structure strongly implies that the dual theory is a $d - 1$ dimensional conformal field theory (CFT), which lives on a sphere at null infinity [8]. Motivated by the triangle equivalence between the soft theorems, memory effects and BMS symmetries [9–15], the celestial holography [16–22] was proposed.[1] This interesting holographic duality argues that the four-dimensional gravity on an asymptotically flat spacetime

is equivalent to a two-dimensional CFT at null infinity, such that the S-matrices of the four-dimensional gravity can be computed from correlation functions in the two-dimensional CFT via a certain Mellin-like transformation, though the precise identification of the dual CFT has remained to be answered.

The codimension two nature of the celestial holography looks mysterious for those who are familiar with normal holographic dualities such as the AdS/CFT. Recently, as a generalization of AdS/CFT, a new type of codimension two holography, called wedge holography, has been found in [27] and studied further in [28,29]. As sketched in Fig. 1, the wedge holography argues that the gravity on a $d + 1$ dimensional wedge region in AdS$_{d+1}$ is dual to a $d - 1$ dimensional CFT on the $d - 1$ dimensional tip of the wedge. We impose the Neumann boundary condition on d dimensional boundaries of the wedge, so called the end of the world branes (EOW branes). We can understand this as a small width limit of the AdS/BCFT [30–32]. Alternatively, we can also understand the wedge holography via a double holography in the light of brane-world holography [33–37] as follows. The $d + 1$ dimensional gravity on the wedge is dual to quantum gravity on the two d dimensional EOW branes via the brane-world holography, which is further dual to a $d - 1$ dimensional CFT on the tip via the standard holography.

Motivated by this, the main purpose of this paper is to explore if we can interpret the celestial holography as an extension of wedge holography to gravity on a flat spacetime. We consider the two new classes of wedge

---

[1]A similar codimension two holography was argued in [23] in the context of eternal inflation. Refer to e.g, [24,25] for a proposal of holographic duality between gravity in four-dimensional Minkowski spacetime and a three-dimensional conformal Carrollian field theory. Also see [26] for a possibility of a codimension one holography between gravity in the $d + 1$ dimensional Euclidean flat space R^{d+1} and a d dimensional CFT on S^d.
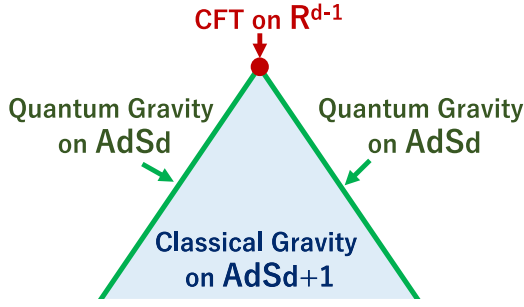
FIG. 1. A sketch of wedge holography, which argues that the gravity on a wedge region in AdS_{d+1} is dual to a $d-1$ dimensional CFT on the codimension two spacetime given by the tip of the wedge.
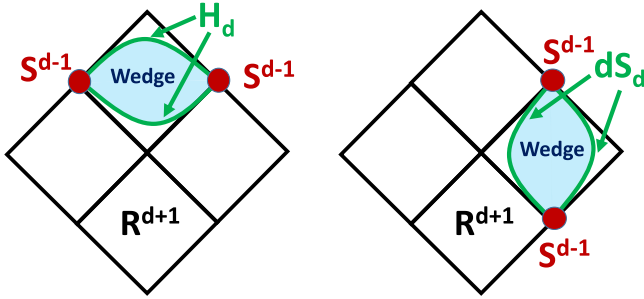

FIG. 2. Sketches of two types of codimension two holographic dualities in flat space. The whole diamond describes a $d+1$ dimensional flat spacetime. The left and right panels describe the hyperbolic and de Sitter sliced wedges (blue regions) surrounded by two end of the world-brane (green surfaces), respectively. We argue that each of them is dual to a CFT on the $d-1$ dimensional sphere (red points).

holography depicted in Fig. 2. One is a hyperbolic sliced wedge region and the other is a de Sitter sliced wedge region, both of which are surrounded by two spacelike or timelike EOW branes, respectively. We argue that each of them is dual to a CFT on the $d-1$ dimensional sphere, situated at the tip of the wedge. The former might be interpreted as a product of lower dimensional AdS/CFT duality for Euclidean AdS geometries, though the product is now taken in the time direction as opposed to the standard wedge holography in [27]. The latter may be regarded as a product of lower dimensional dS/CFT, where the product is taken in the spacial direction.[2] We will examine these new holographic dualities by calculating the entanglement entropy, partition function and two point functions. Finally we will approach the celestial holography by combining these two dualities.

This paper is organized as follows. In Sec. II, we explain hyperbolic and de Sitter slices of Minkowski spacetime and solutions of a free scalar field with a delta functional source

---

[2]For an earlier study of a relation between celestial holography to the dS/CFT refer to [38].

on a sphere at null infinity. In Sec. III, we propose a wedge holography in the hyperbolic patch and present evidence for this duality. In Sec. IV, we propose a wedge holography in the de Sitter patch and present evidence for this. In Sec. V, we will try to interpret the celestial holography by combining the wedge holography in the hyperbolic slices and that in the de Sitter slices. In Sec. VI, we will summarize conclusions and discuss future problems. In appendix A, we briefly present useful identities related to Legendre functions. In appendix B, we describe minimal surfaces and geodesic lengths in hyperbolic spaces. In appendix C, we describe extreme surfaces and geodesic lengths in de Sitter spaces. In appendix D, we present detailed calculations of scalar modes in the de Sitter sliced wedges.

II. HYPERBOLIC AND DE SITTER SLICES OF FLAT SPACETIME

We start from a $d+1$ dimensional flat spacetime $R^{1,d}$:

$$ds^2 = -dT^2 + dR^2 + R^2 d\Omega_{d-1}^2. \tag{2.1}$$

This is decomposed into two patches: the slices of hyperbolic spaces H_d and de Sitter spaces dS_d, which suggest holographic properties [8] (see also [22,39–41]).

The hyperbolic slice is obtained by introducing the new coordinates

$$T = \eta \cosh\rho, \qquad R = \eta \sinh\rho. \tag{2.2}$$

This leads to the metric

$$ds^2 = -d\eta^2 + \eta^2(d\rho^2 + \sinh^2\rho \, d\Omega_{d-1}^2), \quad \text{[hyperbolic patch],} \tag{2.3}$$

On the other hand, the de Sitter slice is introduced by

$$T = r \sinh t, \qquad R = r \cosh t, \tag{2.4}$$

which gives the metric

$$ds^2 = dr^2 + r^2(-dt^2 + \cosh^2 t \, d\Omega_{d-1}^2). \quad \text{[de Sitter patch],} \tag{2.5}$$

In these two patches, the radial coordinates η and r take the values $0 \le \eta < \infty$ and $0 \le r < \infty$. By pasting the two patches along $\eta = 0$ and $r = 0$, we obtain the full four-dimensional Minkowski spacetime as depicted in the left panel of Fig. 3.

We introduce a regularization of the coordinates η and r:

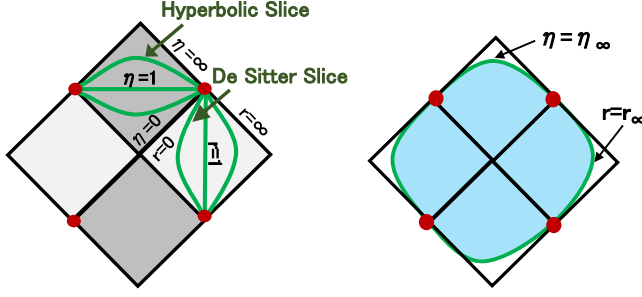$$0 \le \eta \le \eta_\infty, \qquad 0 \le r \le r_\infty. \tag{2.6}$$

FIG. 3. Hyperbolic and de Sitter slices in Minkowski Space (left) and their regularization (right).

This allows us to effectively reduce the hyperbolic patch and the de Sitter patch to H_d and dS_d via the compactification as analogous to the wedge holography for the AdS [27], which is a doubled version of the AdS/BCFT [30,31]. If we extend the wedge holography to the $d + 1$ dimensional Minkowski Space, one may be tempting to argue that a $d - 1$ dimensional CFT on S^{d-1} is dual to the gravity on the $d + 1$ dimensional wedge region (2.6). As usual in the AdS/CFT [3] and the dS/CFT [4], it is useful to introduce the UV cutoff of the dual CFT, which is dual to the geometrical cutoff

$$\rho \leq \rho_\infty, \qquad t \leq t_\infty. \qquad (2.7)$$

Below we will first study the hyperbolic and de Sitter slices separately by considering the wedge holography for each of them. After that we will discuss a connection between the celestial holography and the above wedge holography.

A. Scalar field in hyperbolic patch

Consider perturbations of a real scalar field Ψ in the flat space, which are expected to be dual to scalar operator excitations in the dual CFT on the sphere in our wedge holography. We focus on the four-dimensional gravity case i.e. $d + 1 = 4$ just for simplicity. We write the two-dimensional sphere metric as $d\Omega_2^2 = d\theta^2 + \sin^2\theta d\phi^2$.

We assume a massive free scalar field Ψ given by the action

$$I_{\text{scalar}} = \frac{1}{2} \int dx^4 \sqrt{-g}[-g^{\mu\nu}\partial_\mu\Psi\partial_\nu\Psi - m^2\Psi^2]. \qquad (2.8)$$

The equation of motion reads

$$\frac{1}{\sqrt{-g}}\partial_\mu(\sqrt{-g}g^{\mu\nu}\partial_\nu\Psi) - m^2\Psi = 0. \qquad (2.9)$$

In the hyperbolic patch (2.3), the equation of motion of the scalar field (2.9) is written as (see e.g., [42])

$$-\partial_\eta^2\Psi - \frac{3}{\eta}\partial_\eta\Psi + \frac{1}{\eta^2}(\partial_\rho^2\Psi + 2\coth\rho\partial_\rho\Psi)$$
$$+ \frac{1}{\eta^2\sinh^2\rho}\Delta_2\Psi - m^2\Psi = 0, \qquad (2.10)$$

where Δ_2 is the Laplacian on the two-dimensional sphere. We can solve this by decomposing the solution as follows

$$\Psi(\eta, \rho, \theta, \phi) = f_p(\eta)g_{p,l}(\rho)Y_{lm}(\theta, \phi), \qquad (2.11)$$

where the functions f_p, $g_{p,l}$, and Y_{lm} satisfy

$$\left(-\partial_\eta^2 - \frac{3}{\eta}\partial_\eta + \frac{p^2}{\eta^2} - m^2\right)f_p(\eta) = 0,$$
$$\left(\partial_\rho^2 + 2\coth\rho\partial_\rho - \frac{l(l+1)}{\sinh^2\rho} - p^2\right)g_{p,l} = 0,$$
$$\Delta_2 Y_{lm} = -l(l+1)Y_{lm}. \qquad (2.12)$$

The first equation is explicitly solved as

$$f_p(\eta) = \alpha\frac{I_{\sqrt{1+p^2}}(m\eta)}{\eta} + \beta\frac{K_{\sqrt{1+p^2}}(m\eta)}{\eta}, \qquad (2.13)$$

where α and β are arbitrary constants. The solution to the second one reads

$$g_{p,l}(\rho) = \frac{1}{\sinh\rho} \cdot Q_l^{\sqrt{1+p^2}}(\coth\rho), \qquad (2.14)$$

where Q is the associated Legendre function. We chose Legendre Q function instead of Legendre P function because we require a smooth behavior at $\rho = 0$. Finally the function Y_{lm} is the standard spherical harmonics (A4).

B. Scalar field in de Sitter patch

To obtain the solutions in the de Sitter patch (2.5), we only have to replace the coordinate as

$$\eta = -ir, \qquad \rho = t - \frac{\pi}{2}i. \qquad (2.15)$$

This leads to the solution

$$\Psi(r, t, \theta, \phi) = \tilde{f}_p(r)\tilde{g}_{p,l}(t)Y_{lm}(\theta, \phi), \qquad (2.16)$$

where each function reads

$$\tilde{f}_p(r) = -\alpha e^{\pi i\sqrt{1+p^2}} \cdot \frac{J_{\sqrt{1+p^2}}(mr)}{r}$$
$$- \beta\frac{\pi i}{2}e^{-\pi i\sqrt{1+p^2}} \cdot \frac{H^{(1)}_{\sqrt{1+p^2}}(mr)}{r}, \qquad (2.17)$$

$$\tilde{g}_{p,l}(t) = \frac{1}{\cosh t} \cdot Q_l^{\sqrt{1+p^2}}(\tanh t).\qquad(2.18)$$

Note that if we go from $t = \infty$ to $t = -\infty$, the function $\tilde{g}_{p,l}$ gives the factor $(-1)^l$ because $Q_\nu^\mu(z)$ is given by $z^{-\mu-\nu-1}$ times an even function of z. This explains that the future celestial sphere is related to the past one via the antipodal map $\theta \to \theta + \pi$.

C. Solution with a delta-functional source on the sphere

We input a delta functional source of the scalar field at (θ_0, ϕ_0) on S^2. In the hyperbolic slice, we expand the scalar field in terms of complete set of solutions to the equation of motion for the scalar field by the standard variable separation as in (2.13) and (2.14) under the boundary condition which we are assuming. This leads to the following expansion:

$$\Psi_0^h(\eta, \rho, \theta, \phi) = f_p(\eta) \cdot \frac{\mathcal{N}}{\sinh\rho} \sum_{l=0}^{\infty} \sum_{m=-l}^{l} Y_{lm}^*(\theta_0, \phi_0) Q_l^{\sqrt{1+p^2}}(\coth\rho) Y_{lm}(\theta, \varphi)$$

$$= f_p(\eta) \cdot \frac{\mathcal{N}}{\sinh\rho} \sum_{l=0}^{\infty} \left(\frac{2l+1}{4\pi}\right) P_l(\cos\gamma) Q_l^{\sqrt{1+p^2}}(\coth\rho), \qquad(2.19)$$

where we employed the additivity formula (A7) in the final line and we defined γ by

$$\cos\gamma = \cos\theta_0 \cos\theta + \sin\theta \sin\theta_0 \cos(\varphi - \varphi_0).\quad(2.20)$$

We will choose the normalization factor $\mathcal{N}$ as $\mathcal{N} = e^{-\pi i \sqrt{1+p^2}} \frac{1}{\Gamma(\sqrt{1+p^2})}$.

In the $\rho \to \infty$ limit, using (A3) and (A9), we find

$$\Psi_0^h(\eta, \rho, \theta, \phi) \to f_p(\eta) \cdot \left[e^{(\sqrt{1+p^2}-1)\rho} \delta^2(\Omega - \Omega_0) \right.$$
$$\left. + e^{-(\sqrt{1+p^2}+1)\rho} \frac{\sqrt{1+p^2}}{4\pi} \left(\frac{1-\cos\gamma}{2}\right)^\Delta \right],$$
$$(2.21)$$

which indeed gives the delta-functionally localized source with the correct ρ dependence $e^{(\Delta-d)\rho} = e^{(\sqrt{1+p^2}-1)\rho}$ for a source term in AdS$_3$/CFT$_2$ by identifying the dimension of dual scalar operator Δ as

$$\Delta = 1 + \sqrt{1+p^2}.\qquad(2.22)$$

Moreover, we can show that the full expression of (2.19) is expressed in the form [8]:

$$\Psi_0^h(\eta, \rho, \theta, \phi) = \frac{\Delta-1}{4\pi} \cdot f_p(\eta) \cdot \frac{1}{(\cosh\rho - \cos\gamma \sinh\rho)^\Delta}.$$
$$(2.23)$$

Indeed, we can prove the following expansion:

$$(\cosh\rho - \cos\gamma \sinh\rho)^{-\Delta} = \sum_{l=0}^{\infty} c_l P_l(\cos\gamma), \qquad(2.24)$$

where c_l can be found from the integral formula (A8) as follows:

$$c_l = \frac{e^{-\pi i(\Delta-1)}(2l+1)}{\Gamma(\Delta)} \cdot \frac{1}{\sinh\rho} \cdot Q_l^{\Delta-1}(\coth\rho).\quad(2.25)$$

We can analytically continue the above analysis to the de Sitter slices via the coordinate transformation (2.15).

$$\Psi_0^{ds}(r, t, \theta, \phi) = \tilde{f}_p(r) \cdot \frac{\mathcal{N}}{\cosh t} \sum_{l=0}^{\infty} \left(\frac{2l+1}{4\pi}\right)$$
$$\times P_l(\cos\gamma) Q_l^{\sqrt{1+p^2}}(\tanh\rho). \qquad(2.26)$$

In the $t \to \infty$ limit, we find

$$\Psi_0^{ds}(r, t, \theta, \phi) \to i\tilde{f}_p(r) \cdot \left[e^{(\sqrt{1+p^2}-1)(t-\frac{\pi}{2}i)} \delta^2(\Omega - \Omega_0) \right.$$
$$\left. + e^{-(\sqrt{1+p^2}+1)(t-\frac{\pi}{2}i)} \frac{\sqrt{1+p^2}}{4\pi} \left(\frac{1-\cos\gamma}{2}\right)^\Delta \right].$$
$$(2.27)$$

The full function can be written as

$$\Psi_0^{ds}(r, t, \theta, \phi) = \frac{\Delta-1}{4\pi} e^{\frac{\pi}{2}i(1-\Delta)} \cdot \tilde{f}_p(r)$$
$$\cdot \frac{1}{(\sinh t - \cos\gamma \cosh t + i\tilde{\epsilon})^\Delta}, \qquad(2.28)$$

where $\tilde{\epsilon}$ is the regularization of $i\epsilon$ prescription [8].

III. WEDGE HOLOGRAPHY FOR HYPERBOLIC SLICES

First we consider a wedge holography for hyperbolic slices depicted in the left panel of Fig. 2. We specify the

$d + 1$ dimensional wedge W^h by restricting the coordinate η to the range

$$\eta_1 \leq \eta \leq \eta_2, \tag{3.1}$$

in the coordinate (2.3). We will impose the Neumann boundary condition on the two EOW branes $Q^{h(1)}$ and $Q^{h(2)}$ each at $\eta = \eta_1$ and $\eta = \eta_2$, given by

$$K_{ab} - h_{ab} K = -T h_{ab}, \tag{3.2}$$

where K_{ab} is the extrinsic curvature (we choose the normal vector n^a is out-going) and T is the tension of EOW brane. Indeed we can confirm that the boundary condition (3.2) is satisfied by setting the values of each tension to be

$$T^{h(i)} = \frac{d-1}{d} K^{h(i)} = \frac{d-1}{\eta_i}, \tag{3.3}$$

where $i = 1, 2$ labels the two EOW branes.

By extending the wedge holography in the AdS space [27], we argue that the $d + 1$ dimensional gravity on the wedge W^h (3.1) is dual to a $d - 1$ dimensional CFT on the sphere S^{d-1} at the tip $\rho \to \infty$. We introduce the cutoff $\rho = \rho_\infty$ as in (2.7). Below we will give evidences for this new wedge holography by evaluating the partition function, holographic entanglement entropy and scalar field perturbation. Note that each hyperbolic slice H_d at a fixed value of η has the $SO(1, d)$ symmetry, which is the Lorentz symmetry in the original $d + 1$ dimensional Minkowski spacetime. This symmetry matches with the conformal symmetry of the Euclidean CFT on S^{d-1}. In particular, at $d = 3$, this is enhanced to a pair of Virasoro symmetries, which origins from the superrotation symmetry in $R^{1,3}$, being identified with the conformal symmetry of a dual two-dimensional CFT.

Moreover, the results we will obtain below imply that the dual CFT on S^{d-1} is nonunitary. This is not surprising because we added a timelike interval (3.1) as an internal direction, orthogonal to the hyperbolic space H_d, in spite that we can apply the standard AdS/CFT to each slice. Instead, this is analogous to the dS/CFT, where the dual CFT is expected to be nonunitary based on the analysis of central charge analysis [5] and explicitly known examples of the dS/CFT are nonunitary [43–46].

A. Partition function

The gravity action is written as follows:

$$I_G = \frac{1}{16\pi G_N} \int_{W^h} \sqrt{-g} R + \frac{1}{8\pi G_N} \left[\int_{Q^{h(1)}} \sqrt{\gamma} (K^{h(1)} - T^{h(1)}) \right.$$

$$\left. - \int_{Q^{h(2)}} \sqrt{\gamma} (K^{h(2)} - T^{h(2)}) \right]. \tag{3.4}$$

To evaluate the on-shell action, we note the vanishing curvature $R = 0$ and

$$\int_{Q^{h(i)}} \sqrt{\gamma} = \eta_i^d \omega_{d-1} \int_0^{\rho_\infty} d\rho \sinh^{d-1} \rho, \quad (i = 1, 2), \tag{3.5}$$

where we defined

$$\omega_{d-1} = \frac{d\pi^{\frac{d}{2}}}{\Gamma(\frac{d}{2} + 1)}, \tag{3.6}$$

which is the volume of a unit sphere in $d - 1$ dimension.

By setting,

$$J_d = \int_0^{\rho_\infty} d\rho \sinh^d \rho, \tag{3.7}$$

and plugging (3.3), we obtain on-shell action as follows:

$$I_G = -\frac{1}{8\pi G_N} (\eta_2^{d-1} - \eta_1^{d-1}) \omega_{d-1} J_{d-1}. \tag{3.8}$$

Note that J_d obeys the recursion relation

$$J_d = \frac{1}{d} \sinh^{d-1} \rho_\infty \cosh \rho_\infty - \frac{d-1}{d} J_{d-2}. \tag{3.9}$$

Below we will explicitly evaluate the on-shell action for $d = 3, 4, 5$.

1. $d = 3$ case

When $d = 3$ we explicitly obtain

$$I_G^{d=3} = \frac{\eta_2^2 - \eta_1^2}{16 G_N} (-e^{2\rho_\infty} + 4\rho_\infty). \tag{3.10}$$

By regarding the geometrical cutoff ρ_∞ in H_d as the UV cutoff ϵ in the dual two-dimensional CFT on S^2 by identifying

$$\epsilon = e^{-\rho_\infty}, \tag{3.11}$$

we obtain

$$I_G = -\frac{\eta_2^2 - \eta_1^2}{16 G_N \epsilon^2} - \frac{\eta_2^2 - \eta_1^2}{4 G_N} \log \epsilon. \tag{3.12}$$

This can be comparable to the standard CFT result that the sphere partition function of two-dimensional CFT with the central charge c reads [47,48]

$$Z_{\text{CFT}} \sim e^{\frac{A}{\epsilon^2} - \frac{c}{3} \log \epsilon}, \tag{3.13}$$

where A is nonuniversal constant, while the $\log \epsilon$ term is universal as this is fixed by the conformal anomaly.

By equating this as $Z_{CFT} = e^{iI_G}$, we can estimate the central charge:

$$c = i\frac{3(\eta_2^2 - \eta_1^2)}{4G_N}. \tag{3.14}$$

2. d = 4 case

For $d = 4$, the on-shell action reads

$$I_G = \frac{\eta_2^3 - \eta_1^3}{G_N}\left[-\frac{1}{48}e^{3\rho_\infty} + \frac{3}{16}e^{\rho_\infty}\right] \tag{3.15}$$

Using (3.11), we obtain

$$I_G = -\frac{\eta_2^3 - \eta_1^3}{48G_N\epsilon^3} + \frac{3(\eta_2^3 - \eta_1^3)}{16G_N\epsilon}. \tag{3.16}$$

This is expected to be dual to a three-dimensional CFT. The absence of logarithmic term in the gravity on-shell action is consistent with the well-known fact that there is no conformal anomaly in odd-dimensional CFTs.

3. d = 5 case

For $d = 5$, we obtain

$$I_G = \frac{\pi(\eta_2^4 - \eta_1^4)}{16G_N}\left[-\frac{1}{12}e^{4\rho_\infty} + \frac{2}{3}e^{2\rho_\infty} - 2\rho_\infty\right]. \tag{3.17}$$

In the same way as before, we can rewrite this as follows:

$$I_G = \frac{\pi(\eta_2^4 - \eta_1^4)}{2G_N}\left[-\frac{1}{96\epsilon^4} + \frac{1}{12\epsilon^2} + \frac{1}{4}\log\epsilon\right]. \tag{3.18}$$

Now we would like to compare this result to the CFT one. The 4-sphere partition function with central charges a, c satisfies the following equation [47–49];

$$\begin{aligned}
\epsilon\frac{d}{d\epsilon}\log Z_{CFT} &= -\frac{1}{2\pi}\left\langle\int d^4x\sqrt{g}T_\mu^\mu\right\rangle_{S^4}\\
&= -\frac{1}{2\pi}\int d^4x\sqrt{g}\left(\frac{a}{8\pi}\tilde{R}_{\mu\nu\rho\sigma}R^{\mu\nu\rho\sigma} - \frac{c}{8\pi}W_{\mu\nu\rho\sigma}W^{\mu\nu\rho\sigma}\right)\\
&= -2a\chi(S^4)\\
&= -4a.
\end{aligned} \tag{3.19}$$

In the third line, we use

$$\langle T_\mu^\mu\rangle = \frac{a}{8\pi}\tilde{R}_{\mu\nu\rho\sigma}R^{\mu\nu\rho\sigma} - \frac{c}{8\pi}W_{\mu\nu\rho\sigma}W^{\mu\nu\rho\sigma}. \tag{3.20}$$

And in the fourth line, we use the Euler characteristic class in four-dimensional manifold

$$\frac{1}{32\pi^2}\int d^4x\sqrt{g}\tilde{R}_{\mu\nu\rho\sigma}R^{\mu\nu\rho\sigma} = \chi(M), \tag{3.21}$$

and the fact that the Weyl tensor W vanishes in S^4. By solving (3.19), we obtain the logarithmic part of Z_{CFT},

$$\log Z_{CFT} = 4a\log\epsilon + \text{(other parts)}. \tag{3.22}$$

By equating this as $Z_{CFT} = e^{iI_G}$, we can estimate the central charge:

$$a = i\frac{\pi(\eta_2^4 - \eta_1^4)}{32G_N}. \tag{3.23}$$

B. Holographic entanglement entropy

Now we would like to calculate the holographic entanglement entropy [50–52], which is given by

$$S_A = \frac{\text{Area}(\Gamma_A)}{4G_N}, \tag{3.24}$$

where Γ_A is the extremal surface, which ends on the boundary of A, i.e., $\partial\Gamma_A = \partial A$.

The $d - 1$ dimensional extremal surface[3] which computes the holographic entanglement entropy in our $d + 1$ dimensional wedge W^h is given by a family of the minimal area surfaces in the hyperbolic spaces H_d parametrized by the time coordinate η in the range (3.1). Such an extreme surface is timelike and its area takes a pure imaginary value, as is common to the holographic entanglement entropy in dS/CFT correspondence [46,54,55].

---

[3]Refer to [53] for earlier calculations of entanglement entropy in asymptotically flat spacetime, where the entangling surface lies at null infinity. On the other hand, in our case, we are considering a different quantity, namely the entanglement entropy of two-dimensional CFT on a celestial sphere, where the dual extremal surface extends from the null infinity to the bulk of flat space.

At a fixed value of η, this is given by the standard minimal surface γ_A^H in H_d calculated in Appendix B. We take the metric of H_d to be

$$ds^2 = d\rho^2 + \sinh^2\rho(d\theta_1^2 + \sin^2\theta_1 d\Omega_{d-2}). \quad (3.25)$$

The minimal area which stretches between $\theta = -\theta_0$ to $\theta = \theta_0$ is given by

$$A(\gamma_A^H) = \omega_{d-3} \cdot \int_{\frac{\delta}{L}}^1 dy \frac{(1-y^2)^{\frac{d-4}{2}}}{y^{d-2}}, \quad (3.26)$$

where the infinitesimally small cutoff δ and the minimal surface parameter L, are related to the cutoff ρ_∞ and θ_0 via (B7) and (B8). We again denote the volume of unit d dimensional sphere by ω_d as in (3.6). For $d = 3, 4$ and 5 we obtain the following results:

$$A(\gamma_A^H)_{d=3} = 2\log\frac{2L}{\delta} = 2\log(e^{\rho_\infty}\sin\theta_0),$$

$$A(\gamma_A^H)_{d=4} = 2\pi\left(\frac{L}{\delta} - 1\right) = \pi\sin\theta_0 e^{\rho_\infty} - 2\pi,$$

$$A(\gamma_A^H)_{d=5} = 4\pi\left[\frac{L^2}{2\delta^2} - \frac{1}{2}\log\frac{2L}{\delta} - \frac{1}{4}\right]$$

$$= \frac{\pi}{2}\sin^2\theta_0 e^{2\rho_\infty} - 2\pi\log\left(\frac{\sin\theta_0}{4}e^{\rho_\infty}\right)$$

$$- \pi\cos\theta_0(2 - \cos\theta_0). \quad (3.27)$$

Thus the area of the full extremal surface in W^h is given by

$$A(\Gamma_A^H) = i\int_{\eta_1}^{\eta_2}\eta^{d-1}d\eta \cdot A(\gamma_A^H) = \frac{i}{d-1}(\eta_2^{d-1} - \eta_2^{d-1})A(\gamma_A^H). \quad (3.28)$$

In this way the total expression of the holographic entanglement entropy reads

$$S_A = \frac{A(\Gamma_A^H)}{4G_N} = \frac{i(\eta_2^{d-1} - \eta_1^{d-1})}{4(d-1)G_N}A(\gamma_A^H). \quad (3.29)$$

For $d = 3$ we obtain

$$S_A = \frac{i(\eta_2^2 - \eta_1^2)}{8G_N}\log\left(\frac{\sin^2\theta_0}{\epsilon^2}\right), \quad (3.30)$$

where we employed the relation between the CFT cutoff ϵ and the gravity cutoff ρ_∞ (3.11). We can compare this with the standard result computed in a two-dimensional CFT on S^2 with a central charge c, where

the subsystem A is taken to be an interval; $\theta^{(1)} \le \theta_1 \le \theta^{(2)}$, given by [56,57]:

$$S_A = \frac{c}{6}\log\left[\frac{\sin^2(\frac{\theta^{(1)}-\theta^{(2)}}{2})}{\epsilon^2}\right]. \quad (3.31)$$

This comparison tells us that the central charge takes the following imaginary value

$$c = \frac{3i}{4G_N}(\eta_2^2 - \eta_1^2). \quad (3.32)$$

This agrees with the value (3.14) computed from the partition function.

For $d = 5$ we find by setting $\rho_\infty = -\log\epsilon$ (3.11):

$$S_A = i\frac{\pi(\eta_2^4 - \eta_1^4)}{16G_N}\left[\frac{\sin\theta_0^2}{2\epsilon^2} - 2\log\left(\frac{\sin\theta_0}{4\epsilon}\right)\right.$$

$$\left. - \cos\theta_0(2 - \cos\theta_0)\right]. \quad (3.33)$$

By comparing this with the standard formula in four-dimensional CFTs [51,58]

$$S_A = c_0\epsilon^{-2} + 4a\log\epsilon + O(1), \quad (3.34)$$

we can read off the value of the central charge a:

$$a = \frac{\pi i}{32G_N}(\eta_2^4 - \eta_1^4). \quad (3.35)$$

Indeed this agrees with our previous evaluation from the partition function (3.23).

C. Scalar field perturbation and two point functions

Consider a free massive scalar field in the wedge geometry W^h, defined by $\eta_1 \le \eta \le \eta_2$. We expect this is dual to scalar operators in the dual CFT on S^{d-1}. We impose either the Dirichlet or Neumann boundary condition at the boundary $\eta = \eta_{1,2}$. As we will show below, there are infinitely many scalar modes dual to operators which have conformal dimension $\Delta = 1 + i\lambda_k$ with λ_k real valued. This complex valued conformal dimension again suggests the nonunitary nature of the dual CFT as similar to the celestial holography [17].

1. Dirichlet boundary condition

We impose the Dirichlet boundary condition on the two EOW-branes:

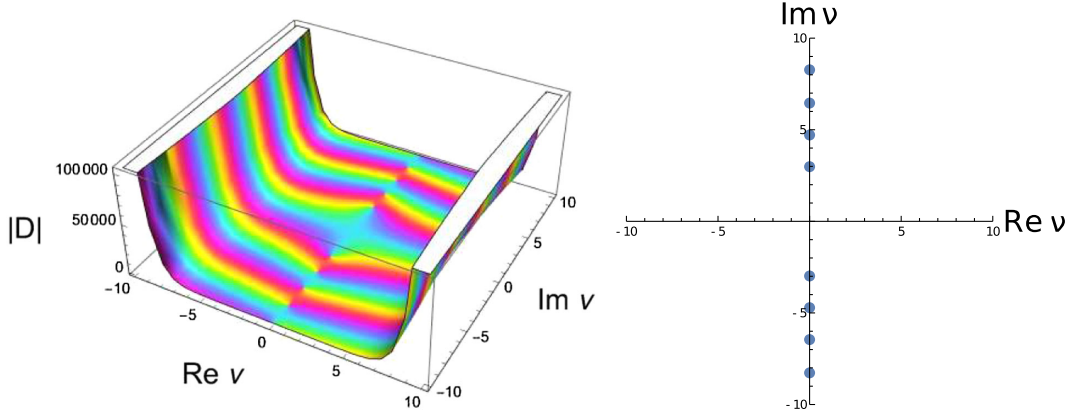$$f_p(\eta_1) = 0, \qquad f_p(\eta_2) = 0, \quad (3.36)$$

FIG. 4. Plots of $D^h(\nu, x_1, x_2)$ for $x_1 = 1$ and $x_2 = 5$ as a function of ν (left) and plots of zero point of D^h (right). The color of left figure represents D's phase.

where the function $f_p(\eta)$ was defined in (2.13). Solving this boundary condition is equivalent to searching for values of $\nu = \sqrt{1 + p^2}$, which satisfy

$$D^h(\nu, x_1, x_2) = I_\nu(x_1)K_\nu(x_2) - I_\nu(x_2)K_\nu(x_1) = 0, \quad (3.37)$$

where $x_{1,2} = m\eta_{1,2}$. Solutions exist only when ν is pure imaginary and there are infinitely many discrete solutions as depicted in Fig. 4. We write the values of ν, which satisfy (3.37) as $\nu = i\lambda_k$. Note that if $\nu = i\lambda_k$ is a solution, then its complex conjugate $\nu = -i\lambda_k$ is also a solution. This shows that a bulk scalar with mass m is dual to infinitely many scalar operators, which have complex and discrete values of conformal dimension:

$$\Delta = 1 + i\lambda_k. \quad (3.38)$$

To see this property analytically, we take two limits: $\eta_2 \to \infty$ and $\eta_1 \to 0$. The first boundary condition can be written as

$$f_p(\eta_2) = \alpha \frac{I_\nu(m\eta_2)}{\eta_2} + \beta \frac{K_\nu(m\eta_2)}{\eta_2} = 0. \quad (3.39)$$

In the limit $\eta_2 \to \infty$, the first term diverges. Thus we must set $\alpha = 0$. In order to satisfy the second condition, we require $\lim_{\eta_1 \to 0} K_\nu(m\eta_1) = 0$. Recalling

$$K_\nu(m\eta) \simeq \frac{\pi}{2} \frac{1}{\sin \nu\pi} \left\{ \frac{\left(\frac{m\eta}{2}\right)^{-\nu}}{\Gamma(1-\nu)} - \frac{\left(\frac{m\eta}{2}\right)^\nu}{\Gamma(1+\nu)} \right\} \quad (0 < \eta \ll 1),$$
$$(3.40)$$

it is obvious that $K_\nu(0)$ diverges if ν has a real part. Thus we set $\nu = i\lambda (\lambda \in \mathbb{R})$.

$$K_{i\lambda}(m\eta) \simeq \frac{\pi}{2} \frac{\frac{e^{-i\lambda \log \frac{m\eta}{2}}}{\Gamma(1-i\lambda)} - \frac{e^{+i\lambda \log \frac{m\eta}{2}}}{\Gamma(1+i\lambda)}}{i \sinh \lambda\pi} = \frac{\pi}{\sinh \lambda\pi} \mathrm{Im}\left(\frac{e^{-i\lambda \log \frac{m\eta}{2}}}{\Gamma(1-i\lambda)} \right).$$
$$(3.41)$$

In the last line we can see that infinitely many (but discrete) values of λ satisfy the necessary condition at nonzero η. We can also see that the satisfactory values of λ become continuous under $\eta \to 0$ because $\log \frac{m\eta}{2} \to -\infty$.

2. Neumann boundary condition

Now we impose the Neumann boundary condition on the two EOW-branes:

$$\partial_\eta f_p(\eta_1) = 0, \qquad \partial_\eta f_p(\eta_2) = 0, \quad (3.42)$$

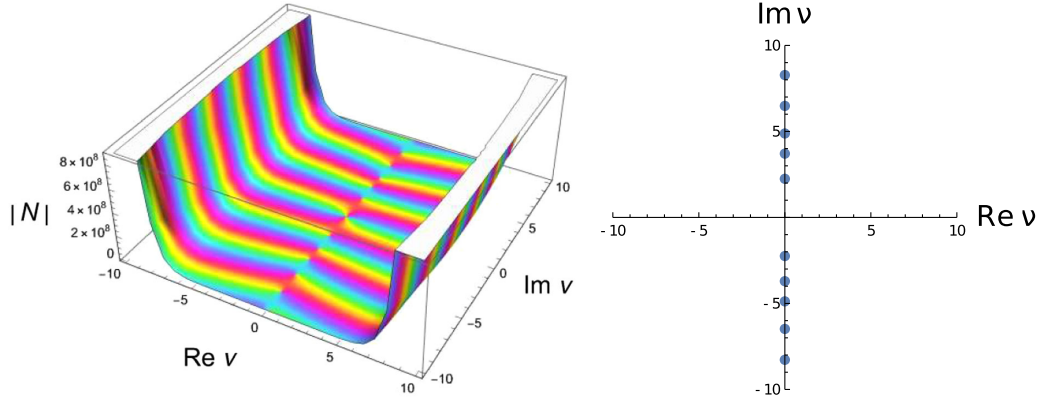where the function $f_p(\eta)$ was defined in (2.13). By using the recurrence formula of modified Bessel function

$$\partial_x I_\nu(x) = \frac{1}{2}(I_{\nu+1}(x) + I_{\nu-1}(x)), \qquad \partial_x K_\nu(x) = -\frac{1}{2}(K_{\nu+1}(x) + K_{\nu-1}(x)),$$
$$\frac{I_\nu(x)}{x} = -\frac{1}{2\nu}(I_{\nu+1}(x) - I_{\nu-1}(x)), \qquad \frac{K_\nu(x)}{x} = \frac{1}{2\nu}(K_{\nu+1}(x) - K_{\nu-1}(x)), \quad (3.43)$$

we can write (3.42) as follows:

FIG. 5.   Plots of $N^h(\nu, x_1, x_2)$ for $x_1 = 1$ and $x_2 = 5$ as a function of ν (left) and plots of zero point of N^h (right). The color of the left figure represents N's phase.

$$\alpha\left(\frac{\nu+1}{2\nu}I_{\nu+1}(m\eta_a) + \frac{\nu-1}{2\nu}I_{\nu-1}(m\eta_a)\right) - \beta\left(\frac{\nu+1}{2\nu}K_{\nu+1}(m\eta_a) + \frac{\nu-1}{2\nu}K_{\nu-1}(m\eta_a)\right) = 0.$$

where $a = 1, 2$. This is equivalent to the search of values of $\nu = \sqrt{1 + p^2}$, which satisfy

$$N^h(\nu, x_1, x_2) = \{(\nu+1)I_{\nu+1}(x_1) + (\nu-1)I_{\nu-1}(x_1)\}\{(\nu+1)K_{\nu+1}(x_2) + (\nu-1)K_{\nu-1}(x_2)\}$$
$$- \{(\nu+1)I_{\nu+1}(x_2) + (\nu-1)I_{\nu-1}(x_2)\}\{(\nu+1)K_{\nu+1}(x_1) + (\nu-1)K_{\nu-1}(x_1)\}$$
$$= 0. \tag{3.44}$$

where $x_{1,2} = m\eta_{1,2}$. Solutions exist only when ν is pure imaginary and there are infinitely many discrete solutions as depicted in Fig. 5. We write the values of ν, which satisfy (3.44) as $\nu = i\lambda_k$. Each mode is dual to a scalar operator with the conformal dimension (3.38). Again, if $\nu = i\lambda_k$ is a solution, then its complex conjugate $\nu = -i\lambda_k$ is also a solution.

We take the limit $\eta_2 \to \infty$ and $\eta_1 \to 0$. The first equation can be written as

$$\partial_\eta f_p(\eta_2) = m\alpha\left(\frac{\nu+1}{2\nu}\frac{I_{\nu+1}(m\eta_2)}{\eta_2} + \frac{\nu-1}{2\nu}\frac{I_{\nu-1}(m\eta_2)}{\eta_2}\right)$$
$$- m\beta\left(\frac{\nu+1}{2\nu}\frac{K_{\nu+1}(m\eta_2)}{\eta_2} + \frac{\nu-1}{2\nu}\frac{K_{\nu-1}(m\eta_2)}{\eta_2}\right)$$
$$= 0. \tag{3.45}$$

In the limit $\eta_2 \to \infty$, the first term diverges. Thus we must take $\alpha = 0$. The second equation can be written as

$$\partial_\eta f_p(\eta_1) = m\beta\left(\frac{\nu+1}{2\nu}\frac{K_{\nu+1}(m\eta_1)}{\eta_1} + \frac{\nu-1}{2\nu}\frac{K_{\nu-1}(m\eta_1)}{\eta_1}\right) = 0. \tag{3.46}$$

In order to satisfy this equation in the limit $\eta_1 \to 0$, it is necessary to impose

$$\lim_{\eta_1 \to 0}\left\{(\nu+1)\frac{K_{\nu+1}(m\eta_1)}{\eta_1} + (\nu-1)\frac{K_{\nu-1}(m\eta_1)}{\eta_1}\right\} = 0. \tag{3.47}$$

In $0 < \eta_1 \ll 1$, applying the asymptotic form (3.40),

(inside the limit)

$$= (\nu+1)\frac{K_{\nu+1}(m\eta_1)}{\eta_1} + (\nu-1)\frac{K_{\nu-1}(m\eta_1)}{\eta_1}$$
$$\simeq -\frac{\pi}{2\sin\nu\pi}\frac{1}{\eta_1}\frac{m}{2}\left\{\frac{(1+\nu)(\frac{m\eta_1}{2})^{-2-\nu}}{\Gamma(-\nu)} + \frac{(1-\nu)(\frac{m\eta_1}{2})^{-2+\nu}}{\Gamma(\nu)}\right\}. \tag{3.48}$$

It is obvious that the last line diverges if ν has a real part. Thus we set $\nu = i\lambda(\lambda \in \mathbb{R})$,

$$(\text{inside the limit}) \simeq -\frac{\pi}{\sin i\lambda\pi}\frac{2}{m\eta_1^2}\text{Re}\left[(1-i\lambda)\frac{e^{i\lambda\log\frac{m\eta_1}{2}}}{\Gamma(i\lambda)}\right]. \tag{3.49}$$

We can see that infinitely many (but discrete) values of λ satisfy the necessary condition at nonzero η_1. We can also see that the satisfactory values of λ become continuous under $\eta_1 \to 0$ because $\log\frac{m\eta_1}{2} \to -\infty$.

3. Two point function

Now let us calculate the two point functions by extending the standard bulk to boundary relation in AdS/CFT [6,7] to our wedge holography. For this we evaluate the on-shell action of scalar field

$$I_{\text{scalar}} = i \int_{\eta_1}^{\eta_2} \frac{d\eta}{\eta} f_p(\eta)^2 \cdot \sinh^2 \rho_\infty \cdot \int d^2 \Omega \Psi \partial_\rho \Psi|_{\rho=\rho_\infty}.$$

(3.50)

Then it is obvious that we obtain the two point function of dual scalar operators at fixed value of p where the product of the first and second term of (2.21) contributes:

$$\langle O_p(\theta_1, \varphi_1) O_p(\theta_2, \varphi_2) \rangle \propto (1 - \cos \gamma_{12})^{-\Delta}, \quad (3.51)$$

where Δ is related to p via (2.22) and we also introduced γ_{12} by

$$\cos \gamma_{12} = \cos \theta_1 \cos \theta_2 + \sin \theta_1 \sin \theta_2 \cos(\varphi_1 - \varphi_2). \quad (3.52)$$

This agrees with the expected two point function of two-dimensional CFT on S^2 by identifying Δ with the conformal dimension of the scalar operator O_p.

IV. WEDGE HOLOGRAPHY FOR DE SITTER SLICES

As the second wedge holography, we consider the $d + 1$ dimensional wedge W^{ds} by restricting the de Sitter sliced metric (2.5) to the region

$$r_1 \le r \le r_2, \quad (4.1)$$

as sketched in the right panel of Fig. 2. The two boundaries $r = r_1$ and $r = r_2$ are the EOW branes $Q^{ds(1)}$ and $Q^{ds(2)}$, where we impose the Neumann boundary condition (3.2). By solving this boundary condition, we obtain

$$T^{ds(i)} = \frac{d-1}{d} K^{ds(i)} = \frac{d-1}{r_i}, \quad (4.2)$$

where $i = 1, 2$ labels the two EOW branes.

We argue that the $d + 1$ dimensional gravity on the wedge W^{ds} (4.1) is dual to a $d - 1$ dimensional CFT on a $d - 1$ dimensional sphere S^{d-1}. Even though two spheres are situated at the tips of the wedge: $t = -\infty$ and $t = \infty$, we identify them via the antipodal mapping. We introduce the cutoff $t = \pm t_\infty$ as in (2.7). As in the hyperbolic case, each de Sitter slice dS_d at a fixed value of r has $SO(1, d)$ symmetry. This is the Lorentz symmetry in the original $d + 1$ dimensional Minkowski spacetime and matches the conformal symmetry of the dual Euclidean CFT on S^{d-1}. At $d = 3$, this is again enhanced to a pair of Virasoro symmetries. This is the superrotation symmetry [59,60]

in $R^{1,3}$ and is identified with the conformal symmetry of a dual two-dimensional CFT.

Notice that this wedge holography can be regarded simply as a dS version of the wedge holography in the AdS [27] because the wedge is defined by adding a spatial width to a dS_d. Therefore we again expect the dual CFT on S^{d-1} is nonunitary being similar to the dS/CFT [4,5,43–46]. We will study the partition function, holographic entanglement entropy and scalar field perturbation to verify this wedge holography.

A. Partition function

The gravity action on our wedge region reads

$$\begin{aligned} I_G = {} & \frac{1}{16\pi G_N} \int_{W^{ds}} \sqrt{-g} R \\ & - \frac{1}{8\pi G_N} \left[\int_{Q^{ds(1)}} \sqrt{-h} (K^{ds(1)} - T^{ds(1)}) \right. \\ & \left. - \int_{Q^{ds(2)}} \sqrt{-h} (K^{ds(2)} - T^{ds(2)}) \right]. \end{aligned}$$

(4.3)

We would like to limit the spacetime to be the half $0 \le t < \infty$. This corresponds to the dual CFT setup where the two spheres at $t = \infty$ and $t = -\infty$ are identified via the antipodal mapping. Also in the absence of this identification, we can obtain the partition function just by doubling it.

By noting

$$\int_{Q^{ds(i)}} \sqrt{-h} = r_i^d \omega_{d-1} \int_0^{t_\infty} dt \cosh^{d-1} t, \quad (4.4)$$

and introducing

$$I_d = \int_0^{t_\infty} dt \cosh^d t, \quad (4.5)$$

we obtain on-shell action as follows:

$$I_G = \frac{1}{8\pi G_N} (r_2^{d-1} - r_1^{d-1}) \omega_{d-1} I_{d-1}. \quad (4.6)$$

We can find the recurrence formula as follows:

$$I_d = \frac{1}{d} \cosh^{d-1} t_\infty \sinh t_\infty + \frac{d-1}{d} I_{d-2}. \quad (4.7)$$

Below we would like to evaluate this explicitly for $d = 3, 4$ and 5.

1. d = 3 case

For $d = 3$, the on-shell action reads

$$I_G = \frac{r_2^2 - r_1^2}{16 G_N} (e^{2t_\infty} + 4t_\infty). \tag{4.8}$$

By regarding the geometrical cutoff t_∞ in the dS$_3$ as the UV cutoff ϵ in the dual two-dimensional CFT on S^2 by identifying

$$\epsilon = e^{-t_\infty}, \tag{4.9}$$

we obtain

$$I_G = \frac{r_2^2 - r_1^2}{16 G_N \epsilon^2} - \frac{r_2^2 - r_1^2}{4 G_N} \log \epsilon. \tag{4.10}$$

By comparing with the standard CFT result (3.13) using the bulk to boundary relation $Z_{\text{CFT}} = e^{iI_G}$, we obtain the central charge c of the dual two-dimensional CFT

$$c = i \frac{3(r_2^2 - r_1^2)}{4 G_N}. \tag{4.11}$$

2. d = 4 case

For $d = 4$, we can evaluate the on-shell action as follows:

$$I_G = \frac{r_2^3 - r_1^3}{G_N} \left[\frac{1}{48} r_\infty^3 e^{3t_\infty} + \frac{3}{8} r_\infty^3 e^{t_\infty} \right] \tag{4.12}$$

Via the relation (4.9), we obtain

$$I_G = \frac{r_2^3 - r_1^3}{48 G_N \epsilon^3} + \frac{3(r_2^3 - r_1^3)}{16 G_N \epsilon}. \tag{4.13}$$

Note that there is no logarithmic term as in odd-dimensions there is no conformal anomaly.

3. d = 5 case

For $d = 5$, we can estimate on-shell action as follows:

$$I_G = \frac{\pi(r_2^4 - r_1^4)}{16 G_N} \left[\frac{1}{12} e^{4t_\infty} + \frac{2}{3} e^{2t_\infty} + 2t_\infty \right]. \tag{4.14}$$

In terms of the CFT cutoff (4.9), we find

$$I_G = \frac{\pi(r_2^4 - r_1^4)}{2 G_N} \left[\frac{1}{96 \epsilon^4} + \frac{1}{12 \epsilon^2} - \frac{1}{4} \log \epsilon \right]. \tag{4.15}$$

By comparing the logarithmic term in $Z_{\text{CFT}} = e^{iI_G}$ with (3.22), we can evaluate

$$a = -i \frac{\pi(r_2^4 - r_1^4)}{32 G_N}. \tag{4.16}$$

B. Holographic entanglement entropy

The extremal surface, which computes the holographic entanglement entropy (3.24) can be constructed from a family of extremal surfaces in the de Sitter slice. Thus, for a fixed value of r, it is given by the extremal surface γ_A^{dS} in dS$_d$ calculated in Appendix C. Consider the metric of dS$_d$ given by

$$ds^2 = -dt^2 + \cosh^2 t (d\theta_1^2 + \sin^2 \theta_1 d\Omega_{d-2}^2). \tag{4.17}$$

The area of an extremal surface, which stretches between $\theta = -\theta_0$ to $\theta = \theta_0$ on the sphere S^{d-1} at the asymptotic boundary $t = t_\infty \to \infty$ is given by

$$A(\gamma_A^{dS}) = i\omega_{d-3} \cdot \int_{\frac{\epsilon}{L}}^{\infty} dy \frac{(1 + y^2)^{\frac{d-4}{2}}}{y^{d-2}}, \tag{4.18}$$

where ϵ and L are related to the cutoff ρ_∞ and θ_0 via (C7) and (C8). Note that this extremal surface is time-like and extends to the other sphere S^{d-1} at $t = -t_\infty \to -\infty$ instead of going back to the original sphere as is typical in the dS/CFT [45,46] (refer to the left panel of Fig. 6). It is also possible to replace $t < 0$ spacetime with an Euclidean flat space:

$$ds^2 = dr^2 + r^2(d\tau^2 + \cos^2 \tau d\Omega_{d-1}^2), \tag{4.19}$$

by performing a Wick rotation $\tau = it$. This provides the Hartle-Hawking construction of the wave function of flat space (refer to the right panel of Fig. 6). In this case, we can connect the extremal surface inside the Euclidean space [45,46]. Motivated by this, we here compute the area of extremal surface for the half of the Lorentzian dS$_d$, i.e., $t \geq 0$. Thus to recover the holographic entanglement
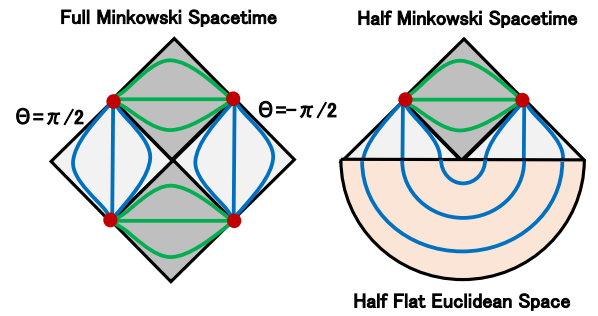

FIG. 6. Sketches of the extremal surfaces, which calculate the holographic entanglement entropy. We chose the maximal subsystem A i.e. $\theta_0 = \frac{\pi}{2}$. The left panel depicts the extremal surfaces in the full Minkowski spacetime. The right one sketches those in the spacetime, which describes the Hartle-Hawking wave function, i.e., a half Euclidean flat space (past) plus a half Minkowski spacetime (future). The green and blue surfaces are the minimal surfaces in the hyperbolic patch and the extremal surfaces in the de Sitter patch, respectively.

entropy for full wedge $-t_\infty < t < t_\infty$, we can simply double the result as in the left panel of Fig. 6. If we would like to consider the holographic entanglement entropy in the Hartle-Hawking state, then we need to add a Euclidean minimal surface area. In this paper, we have in mind the former prescription.

For $d = 3$, 4 and 5 we obtain the following results:

$$A(\gamma_A^{dS})_{d=3} = 2i \log \frac{2L}{\delta} = 2i \log(e^{t_\infty} \sin \theta_0),$$

$$A(\gamma_A^{dS})_{d=4} = 2i\pi \frac{L}{\delta} = \pi i \sin \theta_0 e^{t_\infty},$$

$$A(\gamma_A^{dS})_{d=5} = 4\pi i \left[\frac{L^2}{2\delta^2} + \frac{1}{2} \log \frac{2L}{\delta} + \frac{1}{4} \right]$$

$$= \frac{\pi i}{2} \sin^2 \theta_0 e^{2t_\infty} + 2\pi i \log \left(\frac{\sin \theta_0}{4} e^{t_\infty} \right)$$

$$- \pi i \cos \theta_0 (2 + \cos \theta_0). \tag{4.20}$$

Thus the total area of extremal surface in W^{ds} is given by

$$A(\Gamma_A^{dS}) = \int_{r_1}^{r_2} r^{d-1} dr \cdot A(\gamma_A^{dS}) = \frac{1}{d-1}(r_2^{d-1} - r_1^{d-1}) A(\gamma_A^{dS}). \tag{4.21}$$

In this way the final expression of the holographic entanglement entropy reads

$$S_A = \frac{A(\Gamma_A^{dS})}{4G_N} = \frac{(r_2^{d-1} - r_1^{d-1})}{4(d-1)G_N} A(\gamma_A^{dS}). \tag{4.22}$$

If we consider the Hartle-Hawking prescription of flat space (i.e., the right panel of Fig. 6), we need to add the extra contribution from the extremal surface in Euclidean geometry, denoted by $S_A^{(E)}$. This is computed by setting $A(\gamma_A^{ds})$ to be the area of $d - 2$ dimensional semisphere in (4.22), which leads to

$$S_A^{(E)} = \frac{(r_2^{d-1} - r_1^{d-1})\omega_{d-1}}{8(d-1)G_N}. \tag{4.23}$$

For $d = 3$, we can explicitly evaluate S_A in (4.22) as follows:

$$S_A = \frac{i(r_2^2 - r_1^2)}{8G_N} \log \left(\frac{\sin^2 \theta_0}{\epsilon^2} \right), \tag{4.24}$$

where we employed (4.9). By comparing this with the standard formula (3.31), we can read off the value of the central charge c of the dual two-dimensional CFT:

$$c = \frac{3i}{4G_N}(r_2^2 - r_1^2). \tag{4.25}$$

This agrees with the result (4.11) obtained from the partition function.

For $d = 5$, we obtain

$$S_A = i \frac{\pi(r_2^4 - r_1^4)}{16G_N} \left[\frac{\sin^2 \theta_0}{2\epsilon^2} + 2 \log \left(\frac{\sin \theta_0}{4\epsilon} \right) + O(1) \right]. \tag{4.26}$$

By comparing this with the standard formula in 4D CFT (3.34), we can read off the value of the central charge a:

$$a = -\frac{\pi i(r_2^4 - r_1^4)}{32G_N}. \tag{4.27}$$

Indeed, this reproduces our previous estimation (4.16) from the partition function.

C. Scalar field propagation

Now we consider a free massive scalar field in our wedge geometry W^{ds} defined by $r_1 \leq r \leq r_2$. We again impose the Dirichlet or Neumann boundary condition on the boundary $r = r_{1,2}$. As we will show below, the spectrum of λ_k, where the dual operator dimension reads $\Delta = 1 + i\lambda_k$ consist of the infinitely many real values of λ_k and a finite number of imaginary values of λ_k. The presence of the former, where the conformal dimension (2.22) gets a complex valued, again implies that the dual CFT on S^2 is nonunitary, as in the dS/CFT correspondence. In the dS_3/CFT_2 duality, we find the formula for the conformal dimension $\Delta = 1 \pm \sqrt{1 - M^2}$ [4], where M is the mass of the scalar in the dS_3. If we interpret our wedge holography result in terms of dS_3/CFT_2, we find a finite number of scalar fields in the range $0 < M < 1$ and an infinite number of scalar fields with $M > 1$.

1. Dirichlet boundary condition

Using (2.16) and (2.17), the Dirichlet boundary condition for the scalar reads

$$\tilde{f}_p(r_1) = 0, \qquad \tilde{f}_p(r_2) = 0. \tag{4.28}$$

This is equivalent to find such values of $\nu = \sqrt{1 + p^2}$, which are solutions to

$$D^{ds}(\nu, x_1, x_2) = J_\nu(x_1)H_\nu^{(1)}(x_2) - J_\nu(x_2)H_\nu^{(1)}(x_1) = 0. \tag{4.29}$$

By studying numerically, as plotted in Fig. 7, we find that there is an infinite number of solutions for discrete imaginary values of ν together with a finite number of solutions for real values of ν. In appendix D 1, we analytically explain this behavior of the solutions. We also find that the number of real valued solutions of ν increase as
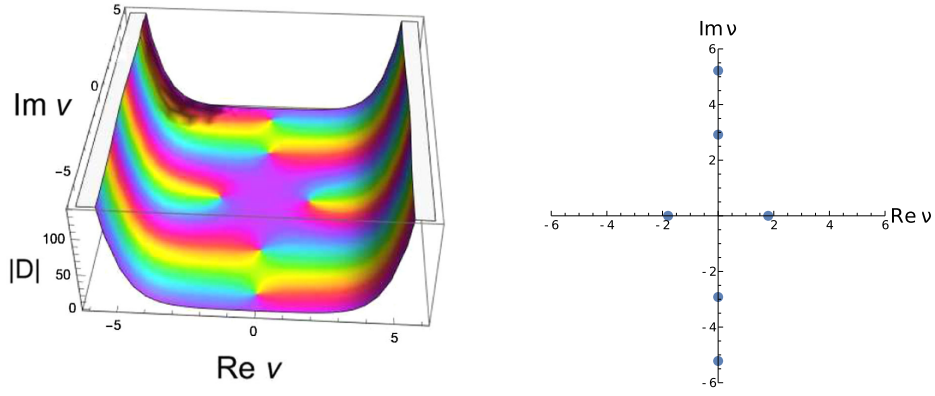
FIG. 7.   Plots of $|D^{dS}(\nu, x_1, x_2)|$ for $x_1 = 1$ and $x_2 = 5$ as a function of ν (left) and plots of zero point of D^{dS} (right). The color of the left figure represents D's phase.

r_2 gets larger and the solutions with imaginary ν become dense in the limit $r_1 \to 0$.

2. Neumann boundary condition

Next, we consider the case that we impose the Neumann boundary condition on the two EOW-branes:

$$\partial_r \tilde{f}_p(r_1) = 0, \qquad \partial_r \tilde{f}_p(r_2) = 0, \qquad (4.30)$$

where the function $\tilde{f}_p(r)$ was defined in (2.17). By using the recurrence formula of the modified Bessel function

$$\partial_x J_\nu(x) = -\frac{1}{2}(J_{\nu+1}(x) - J_{\nu-1}(x)), \qquad \partial_x H_\nu^{(1)}(x) = -\frac{1}{2}(H_{\nu+1}^{(1)}(x) - H_{\nu-1}^{(1)}(x)),$$

$$\frac{J_\nu(x)}{x} = \frac{1}{2\nu}(J_{\nu+1}(x) + J_{\nu-1}(x)), \qquad \frac{H_\nu^{(1)}(x)}{x} = \frac{1}{2\nu}(H_{\nu+1}^{(1)}(x) + H_{\nu-1}^{(1)}(x)), \qquad (4.31)$$

we can write (4.30) as follows:

$$\alpha\left(\frac{\nu+1}{2\nu}J_{\nu+1}(mr_a) - \frac{\nu-1}{2\nu}J_{\nu-1}(mr_a)\right) + m\beta\left(\frac{\nu+1}{2\nu}H_{\nu+1}^{(1)}(mr_a) - \frac{\nu-1}{2\nu}H_{\nu-1}^{(1)}(mr_a)\right) = 0,$$

where $a = 0, 1$. This is equivalent to the search of values of $\nu = \sqrt{1 + p^2}$, which satisfy

$$N^{ds}(\nu, x_1, x_2) = \{(\nu+1)J_{\nu+1}(x_1) - (\nu-1)J_{\nu-1}(x_1)\}\{(\nu+1)H_{\nu+1}^{(1)}(x_2) - (\nu-1)H_{\nu-1}^{(1)}(x_2)\}$$

$$- \{(\nu+1)J_{\nu+1}(x_2) - (\nu-1)J_{\nu-1}(x_2)\}\{(\nu+1)H_{\nu+1}^{(1)}(x_1) - (\nu-1)H_{\nu-1}^{(1)}(x_1)\}$$

$$= 0. \qquad (4.32)$$

where $x_{1,2} = mr_{1,2}$. By studying numerically, as plotted in Fig. 8, we find that there is an infinite number of solutions for discrete values of ν together with a finite number of solutions for real values of ν. The properties of the solutions ν are similar to those in the Dirichlet case. Refer to appendix D 2 for more details.

3. Two point function

We can evaluate the two point functions as we did for the wedge holography in the hyperbolic patch in Sec. III C, by using the scalar field profile (2.27). The result is identical to

(3.51), expect that there are two spheres in the future and past. If we call the operator inserted in the future and past sphere $O_p^{(+)}$ and $O_p^{(-)}$, respectively, then the two point functions read

$$\langle O_p^{(\pm)}(\theta_1, \varphi_1)O_p^{(\pm)}(\theta_2, \varphi_2)\rangle \propto (1 - \cos\gamma_{12})^{-\Delta},$$

$$\langle O_p^{(\pm)}(\theta_1, \varphi_1)O_p^{(\mp)}(\theta_2, \varphi_2)\rangle \propto (1 + \cos\gamma_{12})^{-\Delta}, \qquad (4.33)$$

where γ_{12} was given in (3.52). This means that an operator inserted at a point on the future sphere is equivalent to that inserted at its antipodal point in the past sphere. Under this
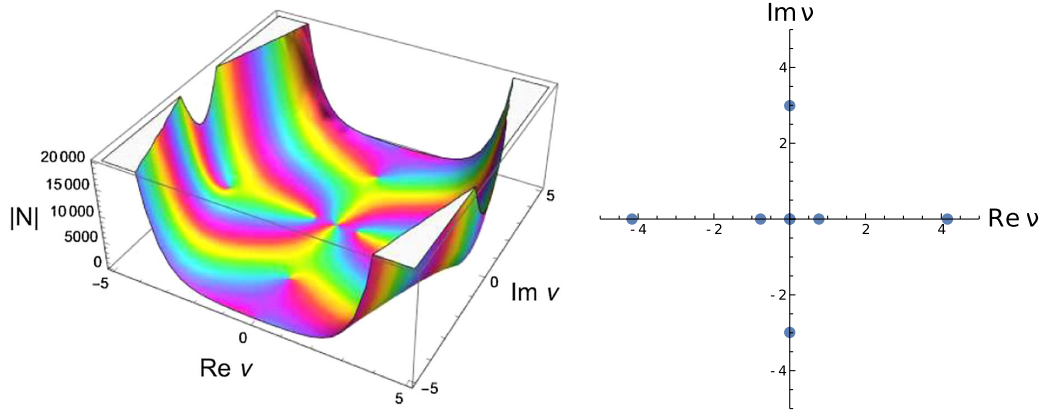
FIG. 8. Plots of $|N^{ds}(\nu, x_1, x_2)|$ for $x_1 = 1$ and $x_2 = 5$ as a function of ν (left) and plots of zero points of N^{ds} (right). The color of the left figure represents N's phase.

identification, the two point functions agree with the CFT expectation.

V. IS CELESTIAL HOLOGRAPHY A WEDGE HOLOGRAPHY?

In the previous sections, we present two new setups of wedge holography in a flat spacetime: hyperbolic slices and de Sitter slices, as explained in Sec. II and depicted in Fig. 2. In this section, we would like to combine these two as in Fig. 3 to approach the celestial holography, which argues that $d + 1$ dimensional gravity in a full Minkowski spacetime is dual to a CFT on the celestial sphere S^{d-1}. As we will see below, as long as we consider the vacuum configurations of celestial holography, it fits nicely with the wedge holography. However, if we consider excitations in celestial holography by gravitational waves, we will see that we must modify the boundary conditions of the flat space wedge holography we considered in the previous section.

A. Partition function in Minkowski spacetime

Let us first calculate the partition function of celestial holography in Minkowski spacetime by regarding the on-shell gravity action as the CFT free energy, simply by extending the standard bulk-boundary relation [6,7] of AdS/CFT. We take the range of η and r to be (2.7). Then, we can simply add up the on-shell actions (3.8) and (4.6) in the wedge holography by setting

$$\eta_2 = \eta_\infty, \qquad r_2 = r_\infty, \qquad \eta_1 = r_1 = 0. \quad (5.1)$$

This leads to

$$I_G = \frac{1}{4\pi G_N} r_\infty^{d-1} \omega_{d-1} I_{d-1} - \frac{1}{4\pi G_N} \eta_\infty^{d-1} \omega_{d-1} J_{d-1}. \quad (5.2)$$

Here, we doubled the result to cover the full Minkowski space, i.e., not only $t > 0$ but also $t < 0$. This is evaluated

in each dimension explicitly. For example, $d = 3, 4, 5$ we obtain

$$d = 3: I_G = \frac{r_\infty^2 - \eta_\infty^2}{8G_N \epsilon^2} - \frac{r_\infty^2 + \eta_\infty^2}{2G_N} \log \epsilon,$$

$$d = 4: I_G = \frac{r_\infty^3 - \eta_\infty^3}{24G_N \epsilon^3} + \frac{3(r_\infty^3 + \eta_\infty^3)}{8G_N \epsilon},$$

$$d = 5: I_G = \frac{\pi(r_\infty^4 - \eta_\infty^4)}{96G_N \epsilon^4} + \frac{\pi(r_\infty^4 + \eta_\infty^4)}{12G_N \epsilon^2} - \frac{\pi(r_\infty^4 - \eta_\infty^4)}{4G_N} \log \epsilon,$$

$$(5.3)$$

where ϵ is the UV cutoff such that $e^{-\rho_\infty} = e^{-t_\infty} = \epsilon$. From the logarithmic terms, we can also read off the values of the central charges c in $d = 3$ and a in $d = 5$ as follows:

$$d = 3: c = i \frac{3(r_\infty^2 + \eta_\infty^2)}{2G_N},$$

$$d = 5: a = i \frac{\pi(\eta_\infty^4 - r_\infty^4)}{16G_N}. \quad (5.4)$$

These are consistent with standard behavior in CFTs except that the central charges take imaginary values, which show that the dual CFT is nonunitary. In our limit $\eta_\infty \to \infty$ and $r_\infty \to \infty$, the two-dimensional CFT central charge becomes $c \to i\infty$. Such a divergent central charge in the dual CFT has also been argued in [22,61]. Moreover, it is intriguing to note that we can have $a = 0$ for the central charge of the four-dimensional CFT if we tune $\eta_\infty = r_\infty$.

B. Holographic entanglement entropy in Minkowski spacetime

We can calculate the holographic entanglement entropy in celestial holography in a Minkowski spacetime. As before, we chose the subsystem A to be $|\theta| \leq \theta_0$ on S^{d-1}. For this, we add the contribution in the hyperbolic patch (3.28) and the de Sitter patch (4.21) of the wedge

holography by taking the range (5.1) and double it to cover the entire spacetime. This leads to the total expression:

$$S_A = \frac{A(\Gamma_A^H) + A(\Gamma_A^{dS})}{4G_N}$$

$$= \frac{i\eta_\infty^{d-1}}{2(d-1)G_N}A(\gamma_A^H) + \frac{r_\infty^{d-1}}{2(d-1)G_N}A(\gamma_A^{dS}). \quad (5.5)$$

For example, we obtain explicit results for $d = 3$ and $d = 5$ as follows:

$$d = 3 : S_A = \frac{i}{4G_N}(\eta_\infty^2 + r_\infty^2) \cdot \log\frac{\sin^2\theta_0}{\epsilon^2},$$

$$d = 5 : S_A = i\frac{\pi(\eta_\infty^4 + r_\infty^4)}{16G_N\epsilon^2} + i\frac{\pi}{4G_N}(r_\infty^4 - \eta_\infty^4)\log\left(\frac{\sin\theta_0}{4\epsilon}\right)$$

$$+ O(1), \quad (5.6)$$

where ϵ is the UV cutoff. By comparing this with the general expressions (3.31) and (3.34), we find the same central charges c and a, which we obtained from the on-shell action in (5.4).

C. Celestial holography versus wedge holography with excitations

The celestial holography [17,42] argues that four-dimensional gravity on the Minkowski spacetime is dual to a two-dimensional CFT on the celestial sphere S^2 at null infinity. One basic relation in the celestial holography is the connection between scattering amplitudes $\mathcal{A}(k_1, k_2, \cdots, k_N)$ of N particles in four-dimensions and correlation functions $\langle O_1 O_2 ... O_N \rangle_{S^2}$ of N primary operators. For a scalar field dual to a scalar operator O_Δ with the dimension Δ, this is explicitly written as follows

$$\langle O_{\Delta_1}(\theta_1, \varphi_1) O_{\Delta_2}(\theta_2, \varphi_2) ... O_{\Delta_N}(\theta_N, \varphi_N) \rangle_{S^2} = \left[\prod_{i=1}^{N} \int dX_i^\mu \phi^{\Delta_i, (\pm)}(X_i^\mu, \theta_i, \varphi_i) \int dk_i^\mu e^{ik_i^\mu X_{\mu i}}\right]\mathcal{A}(k_1, k_2, \cdots, k_N). \quad (5.7)$$

In this correspondence, the functions $\phi^{\Delta_i, (\pm)}$ are called conformal primary wave functions. The superscripts $(+)$ and $(-)$ correspond to out-going and in-coming particle, respectively. They are explicitly given in the following expression [17]:

$$\phi^{\Delta, \pm}(X^\mu, \theta_0, \varphi_0) \equiv \frac{(\sqrt{-X^\mu X_\mu})^{\Delta-1}}{(q^\mu X_\mu^\pm)^\Delta}K_{\Delta-1}(m\sqrt{X^\mu X_\mu}). \quad (5.8)$$

Here X^μ is the four-dimensional Minkowski coordinate, which is related to the hyperbolic patch coordinate and de Sitter patch one via

$$(X^0, X^1, X^2, X^3)|_{X^\mu X_\mu < 0} = \eta \cdot (\cosh\rho, \sinh\rho\sin\theta\cos\phi, \sinh\rho\sin\theta\sin\phi, \sinh\rho\cos\theta),$$

$$(X^0, X^1, X^2, X^3)|_{X^\mu X_\mu > 0} = r \cdot (\sinh t, \cosh t\sin\theta\cos\phi, \cosh t\sin\theta\sin\phi, \cosh t\cos\theta).$$

and q^μ is the null vector

$$(q^0, q^1, q^2, q^3) = \frac{2}{1 + \cos\theta_0}$$

$$\cdot (1, \sin\theta_0\cos\phi_0, \sin\theta_0\sin\phi_0, \cos\theta_0), \quad (5.9)$$

which specifies the direction of particles in the celestial sphere. We also introduced the $i\epsilon$ regularization $X^{\mu, \pm} = X^\mu \pm i\epsilon\{-1, 0, 0, 0\}$.

This wave function $\phi^{\Delta_i, (\pm)}$ can be interpreted as a pointlike excitation on the celestial sphere due to the out-going or in-coming wave. In terms of hyperbolic/de Sitter patch coordinate, the conformal primary wave functions (5.8) read (setting $\epsilon = 0$)

$$\phi^{\Delta, \pm}(X^\mu, \theta_0, \varphi_0)|_{X^\mu X_\mu < 0} = \frac{K_{\Delta-1}(m\eta)}{\eta}\left(\frac{1 + \cos\theta_0}{2}\right)^\Delta$$

$$\times (\cosh\rho - \cos\gamma\sinh\rho)^{-\Delta}, \quad (5.10)$$

$$\phi^{\Delta, \pm}(X^\mu, \theta_0, \varphi_0)|_{X^\mu X_\mu > 0} = -\frac{\pi i}{2}\frac{H_{\Delta-1}^{(a)}(mr)}{r}\left(\frac{1 + \cos\theta_0}{2}\right)^\Delta$$

$$\times (\sinh t - \cos\gamma\cosh t)^{-\Delta}, \quad (5.11)$$

where the type of Hankel function $a = 1, 2$ corresponds to the out-going $(+)$ and in-coming $(-)$ wave. Indeed, these are among the class of the scalar field solutions (2.23) and (2.28) with a delta-functional source on the celestial sphere S^2. In the hyperbolic patch, the celestial holography and our wedge holography discussed in section III have the

same boundary condition for a massive free scalar, i.e., the Dirichlet (or Neumann) boundary condition[4] at $\eta = \eta_\infty$. This is clear from the expression (5.11) as the Bessel function K_ν appears, which exponentially decays as $K_\nu(z) \sim e^{-z}$ for large $|z|$.

However, the boundary condition we impose in the r direction of the de Sitter patch looks different between the celestial holography and our wedge holography. In the former, as in (5.11), we impose the out-going or in-coming boundary condition at $r = r_\infty$, while in the latter we require the Dirichlet (or Neumann) boundary condition. A similar observation is true for the gravitational wave mode, where we impose the out-going or in-coming boundary condition in celestial holography and we do the Neumann boundary condition (3.2) in our wedge holography. In this sense, if we want to interpret the celestial holography in terms of a wedge holography in flat space, we must modify the boundary condition in the de Sitter patch at $r = r_\infty$. However, notice that in the computation of correlation functions, this difference of r dependence only appears in the overall constant and thus does not affect the dependence of celestial sphere coordinate, e.g., in (4.33).

Here, we should also notice that the conformal dimension Δ, available in both hyperbolic patch and de Sitter patch, is $1 + i\lambda$ where λ is an arbitrary real value (see Sec. III C, IV C, Appendix D). This result from our wedge holography is consistent with the principle series in celestial holography, which is constrained from "normalizable condition [18]," not from boundary condition.

VI. CONCLUSIONS AND DISCUSSIONS

In this paper, we proposed extensions of wedge holography to a flat spacetime, largely motivated by the recent developments of celestial holography. A wedge holography [27] is in general codimension two holographic duality between a gravitational theory in a wedge region and a CFT on its tip.

As the first example of wedge holography in a flat spacetime, we argued that a $d + 1$ dimensional region surrounded by two d dimensional hyperbolic spaces (depicted in the left panel of Fig. 2) is dual to a nonunitary CFT on S^{d-1}. We imposed the Neumann boundary condition (3.2) for gravitational modes on the two boundaries, i.e., the end of the world branes (EOW brane). We calculated the on-shell gravity action, holographic entanglement entropy and two point functions in the gravity dual and found that they agree with general expectations in CFTs. The superrotation symmetry at each hyperbolic slice explains the conformal symmetry of the dual Euclidean CFT.

In this example, it is intriguing that a timelike direction, in addition to a space-like radial direction, emerges from the Euclidean CFT. We found that the central charges in even-dimensional CFTs dual to the wedge region take imaginary values and that the conformal dimensions dual to a bulk scalar become complex valued. These two unusual properties show that the dual CFT is nonunitary. This is not at all surprising because there is a good reason to believe that the holographic duality where a real-time direction emerges involves nonunitary theory, as is expected in the dS/CFT duality [4,5]. Indeed, all the known CFT duals of dS/CFT in four-dimensions [43] and in three-dimensions [45] are nonunitary. It will be interesting to explore this wedge holography from a more sophisticated viewpoint such as higher point functions, entanglement wedges and various excited states.

The second example of flat space wedge holography, which we proposed in this paper, is for gravity in the $d + 1$ dimensional wedge region (the right panel of Fig. 2) bounded by two d dimensional de Sitter spaces. We again impose the Neumann boundary condition (3.2) on the two EOW branes. We evaluated the on-shell gravity action, holographic entanglement entropy and two point functions in the gravity dual and again confirmed that they are consistent with general expectations in CFTs. The superrotation symmetry at each de Sitter slice explains the conformal symmetry of the dual Euclidean CFT. This wedge holography can be regarded as a slightly "fatten" version of dS/CFT correspondence by simply adding a spacial interval. Therefore, our calculations and results were parallel with that in dS/CFT. Indeed, the central charges in even-dimensional CFTs on S^{d-1} turned out to take imaginary values. We found that there are infinitely many scalar operators dual to the bulk scalar which have imaginary valued conformal dimensions. In addition, there are a finite number of scalar operators with real valued conformal dimensions.

Since the full Minkowski spacetime can be regarded as a union of the hyperbolic patch and de Sitter patch, we finally considered the possibility that the celestial holography for the former can be interpreted as a combination of the hyperbolic and de Sitter sliced wedge holography. We found that the results of the on-shell action and holographic entanglement for the flat Minkowski spacetime, which are simply the sum of those in hyperbolic and de Sitter sliced wedge holography, look consistent with the CFT expectations. However, if we consider excitations such as the bulk scalar field, we found that the wedge holography in the de Sitter patch has a different boundary condition than that in the celestial holography. The former is either Dirichlet or Neumann and the latter is out-going or in-coming. On the other hand, in the hyperbolic patch, our wedge holography and celestial holography assume the same boundary condition. Therefore, we must modify the usual boundary condition of wedge holography, which is Neumann (3.2)

---

[4]Note that in the UV limit $\eta_\infty \to \infty$ of celestial holography, the Dirichlet and Neumann boundary condition at $\eta = \eta_\infty$ for the scalar field are identical. Thus, we can consider this as the Neumann boundary condition.

for metric perturbation modes, to the out-going or incoming boundary condition to interpret the celestial holography as a wedge holography.

It would be an intriguing future direction to explore more the fundamental mechanism of celestial holography and generalize the flat space holography to nontrivial geometries such as Schwarzschild black holes.

ACKNOWLEDGMENTS

APPENDIX A: USEFUL IDENTITIES OF LEGENDRE FUNCTIONS

The associated Legendre function is defined by (we follow [62])

$$P_\nu^\mu(z) = \frac{1}{\Gamma(1-\mu)}\left(\frac{z+1}{z-1}\right)^{\mu/2} {}_2F_1\left(-\nu, \nu+1; 1-\mu; \frac{1-z}{2}\right).$$

$$Q_\nu^\mu(z) = \frac{e^{\pi\mu i}\sqrt{\pi}\Gamma(\mu+\nu+1)}{2^{\nu+1}\Gamma(\nu+3/2)} z^{-\mu-\nu-1}(z^2-1)^{\mu/2} {}_2F_1\left(\frac{\mu+\nu+2}{2}, \frac{\mu+\nu+1}{2}; \nu+\frac{3}{2}; \frac{1}{z^2}\right). \tag{A1}$$

It is useful to note the asymptotic behavior in the $|z| \to \infty$

$$Q_\nu^\mu(z) \simeq e^{\mu\pi i}\sqrt{\pi}\frac{\Gamma(\nu+\mu+1)}{\Gamma(\nu+3/2)(2z)^{\nu+1}}, \tag{A2}$$

and $z \to 1$

$$Q_\nu^\mu(z) \simeq \frac{e^{\pi\mu i}}{2}\left[\Gamma(\mu)\left(\frac{2}{z-1}\right)^{\mu/2} + \frac{\Gamma(-\mu)\Gamma(\nu+\mu+1)}{\Gamma(\nu-\mu+1)}\left(\frac{z-1}{2}\right)^{\mu/2}\right]. \tag{A3}$$

The spherical harmonic function is defined by

$$Y_{lm}(\theta,\phi) = (-1)^m\sqrt{\frac{(2l+1)(l-m)!}{4\pi(l+m)!}}P_l^m(\cos\theta)e^{im\phi}. \tag{A4}$$

It satisfies the orthonormal condition:

$$\int_0^\pi d\theta \sin\theta \int_0^{2\pi} d\phi Y_{lm}^*(\theta,\phi)Y_{l'm'}(\theta,\phi) = \delta_{ll'}\delta_{mm'}. \tag{A5}$$

We can also show

$$\sum_{l=0}^\infty \sum_{m=-l}^l Y_{lm}^*(\theta,\phi)Y_{lm}(\theta_0,\phi_0)$$
$$= \frac{1}{\sin\theta}\delta(\theta-\theta_0)\delta(\phi-\phi_0) \equiv \delta^2(\Omega-\Omega_0). \tag{A6}$$

The additivity theorem is also useful:

$$Y_{l,0}(\gamma) = \sqrt{\frac{4\pi}{2l+1}}\sum_{m=-l}^l Y_{lm}^*(\theta,\phi)Y_{lm}(\theta_0,\phi_0), \tag{A7}$$

where γ is defined by (2.20).

The following integral formula is also useful (this is Eq.(7.228) of [62])

$$\int_{-1}^1 dx\frac{P_n(x)}{(z-x)^{\mu+1}} = \frac{2}{\Gamma(1+\mu)}(z^2-1)^{-\mu/2}e^{-i\pi\mu}Q_n^\mu(z). \tag{A8}$$

In particular, by taking the limit $z = 1$ we obtain

$$\int_{-1}^1 dx\frac{P_n(x)}{(1-x)^{\mu+1}} = (-1)^n\frac{2^{-\mu}\Gamma(-\mu)^2}{\Gamma(n-\mu+1)\Gamma(-\mu-n)}. \tag{A9}$$

APPENDIX B: MINIMAL SURFACES AND GEODESIC LENGTHS IN H_d

Here we summarize minimal surfaces and geodesic lengths in the hyperbolic space H_d.

1. Minimal surfaces

Consider H_d, whose metric is given by (3.25). This is described by a coordinate $(X_0, X_1, \cdots, X_d)$ on the surface

$$X_0^2 = X_1^2 + \cdots + X_d^2 + 1, \tag{B1}$$

in $R^{1,d}$, via the coordinate transformation:

$$X_0 = \cosh\rho,$$
$$X_1 = \sinh\rho\cos\theta_1,$$
$$X_2 = \sinh\rho\sin\theta_1\cos\theta_2,$$
$$\cdots,$$
$$X_d = \sinh\rho\sin\theta_1\sin\theta_2\cdots\sin\theta_{d-1}. \tag{B2}$$

We can also map this to the Poincaré coordinate as

$$X_0 = \frac{z}{2}\left(1 + \frac{x^2 + 1}{z^2}\right),$$
$$X_1 = -\frac{z}{2}\left(1 - \frac{1 - x^2}{z^2}\right),$$
$$X_i = \frac{x_{i-1}}{z} \quad (i = 2, 3, \cdots, d), \tag{B3}$$

leading to the metric

$$ds^2 = \frac{dz^2 + dx_1^2 + \cdots + dx_{d-1}^2}{z^2}. \tag{B4}$$

It is well known that a class of minimal surfaces in (B4) is given by $d - 2$ dimensional semi-spheres.

$$x_{d-1} = 0,$$
$$z^2 + x_1^2 + \cdots + x_{d-2}^2 = L^2. \tag{B5}$$

In terms of the original coordinate (3.25) of H_d, this is expressed as

$$1 + \sinh^2\rho\sin^2\theta = L^2(\cosh\rho + \sinh\rho\cos\theta_1)^2,$$
$$\theta_{d-1} = 0, \tag{B6}$$

while the angles $(\theta_2, \cdots, \theta_{d-2})$ are free. We introduce θ_0 such that we have $\theta = \pm\theta_0$ at the boundary $\rho = \rho_\infty \to \infty$. This is given by

$$L = \frac{\sin\theta_0}{1 + \cos\theta_0}. \tag{B7}$$

Note also that the cutoff in the Poincaré coordinate $z = \epsilon$ is mapped into that in the original coordinate as

$$\frac{1}{\delta} = \left(\frac{1 + \cos\theta_0}{2}\right)e^{\rho_\infty} + \left(\frac{1 - \cos\theta_0}{2}\right)e^{-\rho_\infty}. \tag{B8}$$

2. Geodesic length

If we consider two points, P_1 and P_2,

$$P_1 = (\rho_1, \theta^{(1)}, \Omega_{d-2}),$$
$$P_2 = (\rho_2, \theta^{(2)}, \Omega_{d-2}). \tag{B9}$$

The geodesic distance D_{12} in the hyperbolic space H_d reads

$$\cosh D_{12} = \cosh\rho_1\cosh\rho_2 - \sinh\rho_1\sinh\rho_2\cos(\theta^{(1)} - \theta^{(2)}). \tag{B10}$$

In the limit $\rho_1 = \rho_2 = \rho_\infty$, this leads to

$$D_{12} = 2\rho_\infty + \log\left(\sin^2\frac{\theta_1 - \theta_2}{2}\right). \tag{B11}$$

The geodesic is explicitly given by

$$\tan\left[\theta - \frac{\theta^{(1)} + \theta^{(2)}}{2}\right] = \frac{1}{\cosh\rho}\sqrt{\frac{\sinh^2\rho}{\sinh^2\rho_*} - 1}, \tag{B12}$$

where we set

$$\tan\left[\frac{\theta^{(1)} - \theta^{(2)}}{2}\right] = \frac{1}{\sinh\rho_*}. \tag{B13}$$

APPENDIX C: EXTREME SURFACES AND GEODESIC LENGTHS IN dS_d

Here, we summarize minimal surfaces and geodesic lengths in the de Sitter spacetime dS_d.

1. Extremal surfaces

Consider dS_d, whose metric is given by (4.17). This is described by a coordinate $(X_0, X_1, \cdots, X_d)$ on the surface

$$X_0^2 + 1 = X_1^2 + \cdots + X_d^2, \tag{C1}$$

in $R^{1,d}$, via the coordinate transformation:

$$X_0 = \sinh t,$$

$$X_1 = \cosh t \cos \theta_1,$$

$$X_2 = \cosh t \sin \theta_1 \cos \theta_2,$$

$$\cdots,$$

$$X_d = \cosh t \sin \theta_1 \sin \theta_2 \cdots \sin \theta_{d-1}. \quad \text{(C2)}$$

We can also map this to the Poincaré coordinate as

$$X_0 = -\frac{z}{2}\left(1 - \frac{x^2 + 1}{z^2}\right),$$

$$X_1 = \frac{z}{2}\left(1 + \frac{1 - x^2}{z^2}\right),$$

$$X_i = \frac{x_{i-1}}{z} \quad (i = 2, 3, \cdots, d), \quad \text{(C3)}$$

leading to the metric

$$ds^2 = \frac{-dz^2 + dx_1^2 + \cdots + dx_{d-1}^2}{z^2}. \quad \text{(C4)}$$

It is well known that a class of minimal surfaces in (C4) is given by $d - 2$ dimensional semispheres.

$$x_{d-1} = 0,$$

$$x_1^2 + \cdots + x_{d-2}^2 = z^2 + L^2. \quad \text{(C5)}$$

In terms of the original coordinate (4.17) of dS_d, this is expressed as

$$\cosh^2 t \sin^2 \theta = L^2(\sinh t + \cosh t \cos \theta_1)^2 + 1,$$

$$\theta_{d-1} = 0, \quad \text{(C6)}$$

while the angles $(\theta_2, \cdots, \theta_{d-2})$ are free. We introduce θ_0 such that we have $\theta = \pm\theta_0$ at the boundary $\rho = \rho_\infty \to \infty$. This is given by

$$L = \frac{\sin \theta_0}{1 + \cos \theta_0}. \quad \text{(C7)}$$

Note also that the cutoff in the Poincaré coordinate $z = \delta$ is mapped into that in the original coordinate as

$$\frac{1}{\delta} = \left(\frac{1 + \cos \theta_0}{2}\right)e^{t_\infty} - \left(\frac{1 - \cos \theta_0}{2}\right)e^{-t_\infty}. \quad \text{(C8)}$$

2. Geodesic length

If we choose two points, P_1 and P_2, on dS_d:

$$P_1 = (t_1, \theta^{(1)}, \Omega_{d-2}),$$

$$P_2 = (t_2, \theta^{(2)}, \Omega_{d-2}), \quad \text{(C9)}$$

where we took the locations on S^{d-2} are the same without losing generality owing to the $SO(d-1)$ symmetry. The geodesic distance between P_1 and P_2, denoted by D_{12}, can be found as

$$\cos D_{12} = \cos(\theta^{(1)} - \theta^{(2)}) \cosh t_1 \cosh t_2 - \sinh t_1 \sinh t_2.$$
$$\text{(C10)}$$

If we choose $t_1 = t_2 = t_\infty \to \infty$, we find

$$D_{12} \simeq 2it_\infty + i \log\left[\sin^2\left(\frac{\theta^{(1)} - \theta^{(2)}}{2}\right)\right] + \pi. \quad \text{(C11)}$$

The imaginary divergent contribution comes from the timelike geodesic and the final real part π is from the geodesic in an Euclidean space (d dim. half sphere). For more details of this and an interpretation in dS/CFT, refer to Fig. 5 of [46].

On the other hand, if we choose $t_1 = -t_2 = t_\infty \to \infty$, we obtain

$$D_{12} \simeq 2it_\infty + i \log\left[\cos^2\left(\frac{\theta^{(1)} - \theta^{(2)}}{2}\right)\right]. \quad \text{(C12)}$$

Note that if we replace θ_2 with the antipodal one $\theta_2 + \pi$, then we get the behavior of (C11).

APPENDIX D: SCALAR FIELD MODES IN DE SITTER SLICED WEDGES

Here, we present analytical calculations of scalar field modes, which satisfy either the Dirichlet or Neumann boundary condition in the de Sitter sliced wedges $r_1 \leq r \leq r_2$. In Figs. 9–12, D and N are defined as (4.29), (4.32).

1. Dirichlet boundary condition

As opposed to the hyperbolic slice case, the values of ν satisfying the boundary condition can also be real as well as pure imaginary. We can rewrite (2.17) as following:

$$\tilde{f}(r) = \alpha \frac{H_\nu^{(1)}(mr)}{r} + \beta \frac{H_\nu^{(2)}(mr)}{r}. \quad \text{(D1)}$$

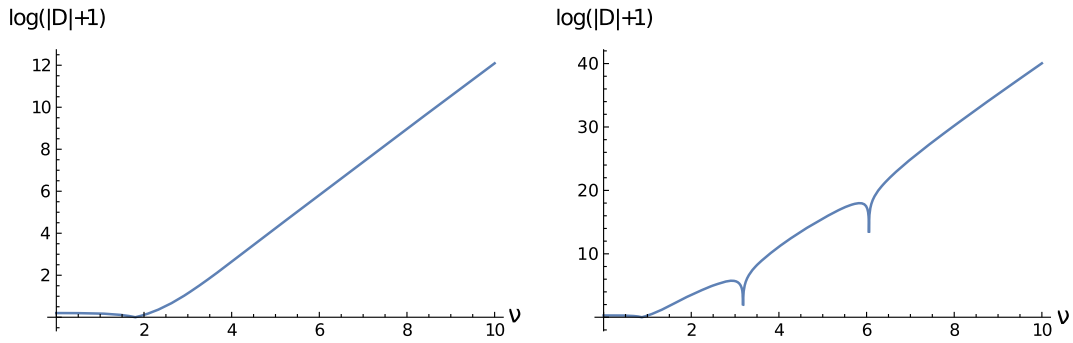Then, the boundary condition (4.28) can be written as

FIG. 9. Plots of $\log(|D(\nu, x_1, x_2)| + 1)$ for $x_1 = 1$ and $x_2 = 5$ as a function of real ν (left) and plots for $x_1 = 0.1$ and $x_2 = 10$ (right). The downward pointing part of the graph indicates the zero point of D.
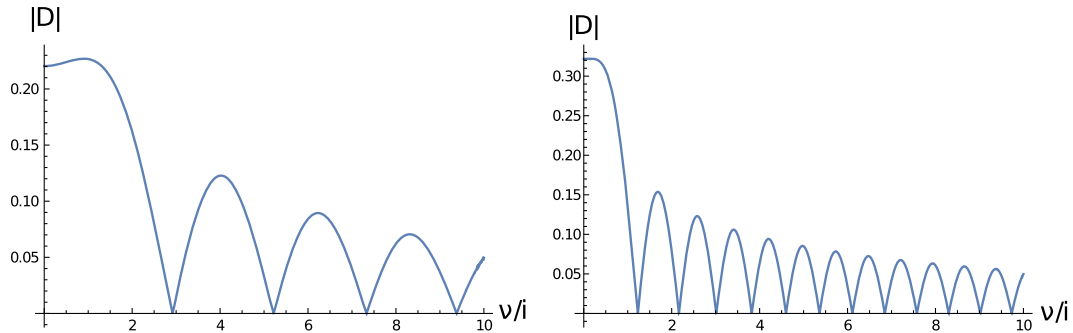

FIG. 10. Plots of $|D(\nu, x_1, x_2)|$ for $x_1 = 1$ and $x_2 = 5$ as a function of imaginary ν (left) and plots for $x_1 = 0.1$ and $x_2 = 10$ (right).
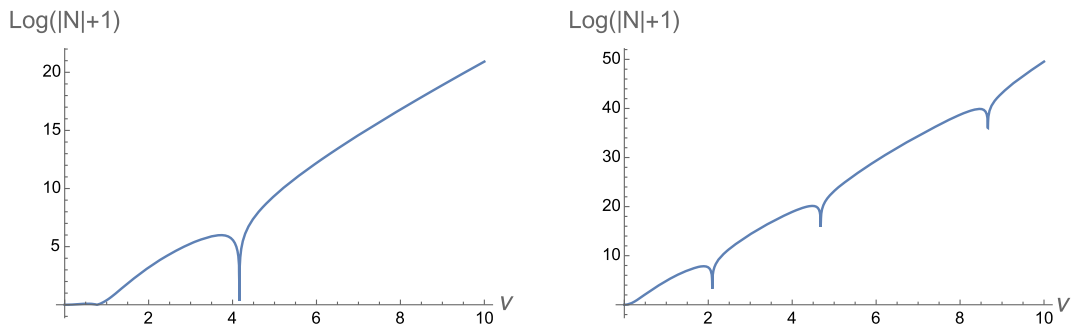

FIG. 11. Plots of $\log(|N(\nu, x_1, x_2)| + 1)$ for $x_1 = 1$ and $x_2 = 5$ as a function of real values of ν (left) and plots for $x_1 = 0.1$ and $x_2 = 10$ (right). The downward pointing part of the graph indicates the zero point of N.
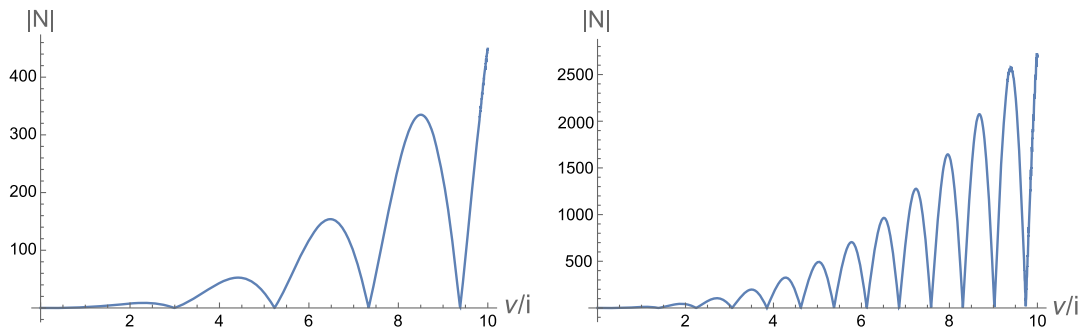

FIG. 12. Plots of $N^{dS}(\nu, x_1, x_2)$ for $x_1 = 1$ and $x_2 = 5$ as a function of imaginary values of ν (left) and plots for $x_1 = 0.1$ and $x_2 = 10$ (right).

$$\tilde{f}(r_i) = 0 \Leftrightarrow \alpha H_\nu^{(1)}(x_i) + \beta H_\nu^{(2)}(x_i) = 0$$

$$\Leftrightarrow \tilde{\alpha} = -\frac{H_\nu^{(2)}(x_i)}{H_\nu^{(1)}(x_i)} = \frac{e^{i\nu\pi}J_\nu(x_i) - J_{-\nu}(x_i)}{e^{-i\nu\pi}J_\nu(x_i) - J_{-\nu}(x_i)} \quad \text{(D2)}$$

where $x_i = mr_i$, $i = 1, 2$ and $\tilde{\alpha} = \frac{\alpha}{\beta}$. Note that by flipping the sign of ν, we obtain

$$\tilde{\alpha}(-\nu) = e^{-2\nu\pi i}\tilde{\alpha}(\nu), \quad \text{(D3)}$$

which leads us to conclude that if ν satisfies the boundary condition (D2), $-\nu$ also satisfies the condition. From the

viewpoint of the numerical result, it would be sufficient to focus on only real ν and/or pure imaginary ν case. Before we proceed to the detailed analysis, let us review the asymptotic form of the Hankel functions. In the limit $|z| \to \infty$,

$$H_\nu^{(1)}(z) \sim \sqrt{\frac{2}{\pi z}} e^{i(z - \frac{2\nu+1}{4}\pi)}, \quad H_\nu^{(2)}(z) \sim \sqrt{\frac{2}{\pi z}} e^{-i(z - \frac{2\nu+1}{4}\pi)}. \quad \text{(D4)}$$

Also, in the region $z \sim \nu \to \infty$,

$$H_\nu^{(1)}(a\nu) = \begin{cases} -i\sqrt{\frac{2}{\pi\nu\tanh\alpha}} e^{\nu(\alpha - \tanh\alpha)}(1 + O(\nu^{-1/5})) & [a = \operatorname{sech}\alpha < 1] \\ -\frac{1}{3\pi}\Gamma(\frac{1}{3})(e^{5\pi i/6} + i)(\frac{6}{\nu})^{1/3}(1 + O(\nu^{-1/4})) & [a = 1] \\ -e^{3\pi i/4}\sqrt{\frac{2}{\pi\nu\tan\alpha}} e^{i\nu(\tan\alpha - \alpha)}(1 + O(\nu^{-1/5})) & [a = \sec\alpha > 1] \end{cases} \quad \text{(D5)}$$

$$H_\nu^{(2)}(a\nu) = \begin{cases} i\sqrt{\frac{2}{\pi\nu\tanh\alpha}} e^{\nu(\alpha - \tanh\alpha)}(1 + O(\nu^{-1/5})) & [a = \operatorname{sech}\alpha < 1] \\ -\frac{1}{3\pi}\Gamma(\frac{1}{3})(e^{-5\pi i/6} - i)(\frac{6}{\nu})^{1/3}(1 + O(\nu^{-1/4})) & [a = 1] \\ -e^{-3\pi i/4}\sqrt{\frac{2}{\pi\nu\tan\alpha}} e^{-i\nu(\tan\alpha - \alpha)}(1 + O(\nu^{-1/5})) & [a = \sec\alpha > 1]. \end{cases} \quad \text{(D6)}$$

First, we consider the positive real ν case (remember that sign-flipped νs are also solution). We would like to estimate $\tilde{\alpha}$ in $x_2 \to \infty$, $x_1 \to 0$. Taking x_2 large, we can write $\tilde{\alpha}$ as following:

$$\tilde{\alpha} = -\frac{H_\nu^{(2)}(x_2)}{H_\nu^{(1)}(x_2)}$$

$$\sim \begin{cases} -e^{-i\{2x_2 - (\nu + \frac{1}{2})\pi\}} & (x_2 \gg |\nu|) \\ -1 & (x_2 < |\nu|). \end{cases} \quad \text{(D7)}$$

And, in small x_1, we can write $\tilde{\alpha}$ as following:

$$\tilde{\alpha} = \frac{e^{i\nu\pi}J_\nu(x_i) - J_{-\nu}(x_i)}{e^{-i\nu\pi}J_\nu(x_i) - J_{-\nu}(x_i)}$$

$$\sim \frac{e^{i\nu\pi}\gamma(\frac{x_1}{2})^\nu - (\frac{x_1}{2})^{-\nu}}{e^{-i\nu\pi}\gamma(\frac{x_1}{2})^\nu - (\frac{x_1}{2})^{-\nu}} \quad \text{(D8)}$$

where $\gamma \equiv \frac{\Gamma(1-\nu)}{\Gamma(1+\nu)}$. When we take ν as positive real, we can solve (D2) as

$$-e^{-i\{2x_2 - (\nu + \frac{1}{2})\pi\}} \sim -1 \quad (\nu \ll x_2) \quad \text{(D9)}$$

$$-1 \sim 1 \quad (\nu > x_2). \quad \text{(D10)}$$

In the $\nu < x_2$ region, there exist solutions of ν with a period of approximately 2. Obviously, there are no solutions in the $\nu > x_2$ region. Thus, we conclude that there are finitely many solutions of real ν and the number of real solutions is bounded by x_2. This result is consistent with the numerical calculations, depicted in Fig. 9.

Next, we take ν as pure imaginary $\nu = i\lambda$ and focus on the positive λ case. The conditions (D7) and (D8) are also valid, even if ν is pure imaginary. We would like to estimate $\tilde{\alpha}$ in $x_2 \to \infty$, $x_1 \to 0$. Taking x_2 large, we can write $\tilde{\alpha}$ as following:

$$\tilde{\alpha} = -\frac{H_\nu^{(2)}(x_2)}{H_\nu^{(1)}(x_2)}$$

$$\sim -e^{-i(2x_2 - \frac{1}{2}\pi)} e^{-\lambda\pi}. \quad \text{(D11)}$$

We can see $|\tilde{\alpha}| \sim e^{-\lambda\pi}$. In small x_1, we can write $\tilde{\alpha}$ as following:

$$\tilde{\alpha} = \frac{e^{i\nu\pi}J_\nu(x_i) - J_{-\nu}(x_i)}{e^{-i\nu\pi}J_\nu(x_i) - J_{-\nu}(x_i)}$$

$$\sim \frac{e^{-\lambda\pi}\gamma(\frac{x_1}{2})^{i\lambda} - (\frac{x_1}{2})^{-i\lambda}}{e^{\lambda\pi}\gamma(\frac{x_1}{2})^{i\lambda} - (\frac{x_1}{2})^{-i\lambda}} \quad \text{(D12)}$$

Then, at large λ, we can also see $|\tilde{\alpha}| \sim e^{-\lambda\pi}$. Therefore, we must focus on the phase matching of $\tilde{\alpha}$ in both limits.

$$e^{\lambda\pi}\tilde{\alpha} = \frac{-(\gamma^{\frac{1}{2}}(\frac{x_1}{2})^{i\lambda} - e^{\lambda\pi}\gamma^{-\frac{1}{2}}(\frac{x_1}{2})^{-i\lambda})^2}{|e^{\lambda\pi}\gamma(\frac{x_1}{2})^{i\lambda} - (\frac{x_1}{2})^{-i\lambda}|^2} \qquad (D13)$$

After a little calculation, we obtain

$$\frac{\text{Im}[-\tilde{\alpha}^{1/2}]}{\text{Re}[-\tilde{\alpha}^{1/2}]} = -\frac{1}{\tanh\frac{\lambda\pi}{2}}\tan\left(\lambda\log\frac{x_1}{2} + \theta\right) \qquad (D14)$$

where $\gamma^{\frac{1}{2}} \equiv e^{i\theta}$. From (D11),

$$\frac{\text{Im}[-\tilde{\alpha}^{1/2}]}{\text{Re}[-\tilde{\alpha}^{1/2}]} = -\tan\left(x_1 - \frac{1}{4}\pi\right) \qquad (D15)$$

We can see that infinitely many (but discrete) values of λ yields $\tilde{f}$ satisfying the Dirichlet boundary condition. We can also see that the satisfactory values of λ become continuous under $x_1 \to 0$ because $\log\frac{x_1}{2} \to -\infty$. This result is consistent with the numerical calculations, depicted in Fig. 10.

2. Neumann boundary condition

From Fig. 11, we can observe the emergence of new zero points on the real axis of ν under the limits $r_2 \to \infty$ and $r_1 \to 0$. And from Fig. 12, we can see that the gap of each zero point of D^{ds} on the imaginary axis of ν decreases as r_2 approaches to ∞ and r_1 to 0. From the same calculation in the Dirichlet boundary condition, we can show this numerically.

[1] G. 't Hooft, Dimensional reduction in quantum gravity, Conf. Proc. C **930308**, 284 (1993).

[2] L. Susskind, The world as a hologram, J. Math. Phys. (N.Y.) **36**, 6377 (1995).

[3] J. M. Maldacena, The large N limit of superconformal field theories and supergravity, Adv. Theor. Math. Phys. **2**, 231 (1998).

[4] A. Strominger, The dS/CFT correspondence, J. High Energy Phys. 10 (2001) 034.

[5] J. M. Maldacena, Non-Gaussian features of primordial fluctuations in single field inflationary models, J. High Energy Phys. 05 (2003) 013.

[6] S. S. Gubser, I. R. Klebanov, and A. M. Polyakov, Gauge theory correlators from noncritical string theory, Phys. Lett. B **428**, 105 (1998).

[7] E. Witten, Anti-de Sitter space and holography, Adv. Theor. Math. Phys. **2**, 253 (1998).

[8] J. de Boer and S. N. Solodukhin, A holographic reduction of Minkowski space-time, Nucl. Phys. **B665**, 545 (2003).

[9] A. Strominger, On BMS invariance of gravitational scattering, J. High Energy Phys. 07 (2014) 152.

[10] T. He, V. Lysov, P. Mitra, and A. Strominger, BMS supertranslations and Weinberg's soft graviton theorem, J. High Energy Phys. 05 (2015) 151.

[11] T. He, P. Mitra, A. P. Porfyriadis, and A. Strominger, New symmetries of massless QED, J. High Energy Phys. 10 (2014) 112.

[12] A. Strominger and A. Zhiboedov, Gravitational memory, BMS supertranslations and soft theorems, J. High Energy Phys. 01 (2016) 086.

[13] S. Pasterski, Asymptotic symmetries and electromagnetic memory, J. High Energy Phys. 09 (2017) 154.

[14] A. Strominger, Lectures on the infrared structure of gravity and gauge theory, arXiv:1703.05448.

[15] F. Capone, K. Nguyen, and E. Parisini, Charge and antipodal matching across spatial infinity, arXiv:2204.06571.

[16] T. He, P. Mitra, and A. Strominger, 2D Kac-Moody symmetry of 4D Yang-Mills theory, J. High Energy Phys. 10 (2016) 137.

[17] S. Pasterski, S.-H. Shao, and A. Strominger, Flat space amplitudes and conformal symmetry of the celestial sphere, Phys. Rev. D **96**, 065026 (2017).

[18] S. Pasterski and S.-H. Shao, Conformal basis for flat space amplitudes, Phys. Rev. D **96**, 065022 (2017).

[19] S. Pasterski, S.-H. Shao, and A. Strominger, Gluon amplitudes as 2d conformal correlators, Phys. Rev. D **96**, 085006 (2017).

[20] A. Bagchi, R. Basu, A. Kakkar, and A. Mehra, Flat holography: Aspects of the dual field theory, J. High Energy Phys. 12 (2016) 147.

[21] C. Cardona and Y.-t. Huang, S-matrix singularities and CFT correlation functions, J. High Energy Phys. 08 (2017) 133.

[22] C. Cheung, A. de la Fuente, and R. Sundrum, 4D scattering amplitudes and asymptotic symmetries from 2D CFT, J. High Energy Phys. 01 (2017) 112.

[23] B. Freivogel, Y. Sekino, L. Susskind, and C.-P. Yeh, A holographic framework for eternal inflation, Phys. Rev. D **74**, 086003 (2006).

[24] C. Dappiaggi, BMS field theory and holography in asymptotically flat space-times, J. High Energy Phys. 11 (2004) 011.

[25] L. Donnay, A. Fiorucci, Y. Herfray, and R. Ruzziconi, A Carrollian Perspective on Celestial Holography, Phys. Rev. Lett. **129**, 071602 (2022).

[26] W. Li and T. Takayanagi, Holography and Entanglement in Flat Spacetime, Phys. Rev. Lett. **106**, 141301 (2011).

[27] I. Akal, Y. Kusuki, T. Takayanagi, and Z. Wei, Codimension two holography for wedges, Phys. Rev. D **102**, 126007 (2020).

[28] R.-X. Miao, An exact construction of codimension two holography, J. High Energy Phys. 01 (2021) 150.

[29] R.-X. Miao, Codimension-n holography for cones, Phys. Rev. D **104,** 086031 (2021).

[30] T. Takayanagi, Holographic Dual of BCFT, Phys. Rev. Lett. **107,** 101602 (2011).

[31] M. Fujita, T. Takayanagi, and E. Tonni, Aspects of AdS/ BCFT, J. High Energy Phys. 11 (2011) 043.

[32] A. Karch and L. Randall, Open and closed string interpretation of SUSY CFT's on branes with boundaries, J. High Energy Phys. 06 (2001) 063.

[33] L. Randall and R. Sundrum, A Large Mass Hierarchy from a Small Extra Dimension, Phys. Rev. Lett. **83,** 3370 (1999).

[34] L. Randall and R. Sundrum, An Alternative to Compactification, Phys. Rev. Lett. **83,** 4690 (1999).

[35] S. S. Gubser, AdS/CFT and gravity, Phys. Rev. D **63,** 084017 (2001).

[36] A. Karch and L. Randall, Locally localized gravity, J. High Energy Phys. 05 (2001) 008.

[37] A. Almheiri, R. Mahajan, J. Maldacena, and Y. Zhao, The page curve of Hawking radiation from semiclassical geometry, J. High Energy Phys. 03 (2020) 149.

[38] C. Liu and D. A. Lowe, Conformal wave expansions for flat space amplitudes, J. High Energy Phys. 07 (2021) 102.

[39] A. Ball, E. Himwich, S. A. Narayanan, S. Pasterski, and A. Strominger, Uplifting AdS_3/CFT_2 to flat space holography, J. High Energy Phys. 08 (2019) 168.

[40] K. Nguyen, Schwarzian transformations at null infinity or the unobservable sector of celestial holography, *Proc. Sci.*, CORFU2021 (2022) 133 [arXiv:2201.09640].

[41] L. Donnay, K. Nguyen, and R. Ruzziconi, Loop-corrected subleading soft theorem and the celestial stress-tensor, J. High Energy Phys. 09 (2022) 063.

[42] A.-M. Raclariu, Lectures on celestial holography, arXiv:2107.02075.

[43] D. Anninos, T. Hartman, and A. Strominger, Higher spin realization of the dS/CFT correspondence, Classical Quantum Gravity **34,** 015009 (2017).

[44] J. Cotler, K. Jensen, and A. Maloney, Low-dimensional de Sitter quantum gravity, J. High Energy Phys. 06 (2020) 048.

[45] Y. Hikida, T. Nishioka, T. Takayanagi, and Y. Taki, Holography in de Sitter Space via Chern-Simons Gauge Theory, Phys. Rev. Lett. **129,** 041601 (2022).

[46] Y. Hikida, T. Nishioka, T. Takayanagi, and Y. Taki, CFT duals of three-dimensional de Sitter gravity, J. High Energy Phys. 05 (2022) 129.

[47] M. J. Duff, Twenty years of the Weyl anomaly, Classical Quantum Gravity **11,** 1387 (1994).

[48] M. Henningson and K. Skenderis, The holographic Weyl anomaly, J. High Energy Phys. 07 (1998) 023.

[49] J. L. Cardy, Is there a c theorem in four-dimensions?, Phys. Lett. B **215,** 749 (1988).

[50] S. Ryu and T. Takayanagi, Holographic Derivation of Entanglement Entropy from AdS/CFT, Phys. Rev. Lett. **96,** 181602 (2006).

[51] S. Ryu and T. Takayanagi, Aspects of holographic entanglement entropy, J. High Energy Phys. 08 (2006) 045.

[52] V. E. Hubeny, M. Rangamani, and T. Takayanagi, A covariant holographic entanglement entropy proposal, J. High Energy Phys. 07 (2007) 062.

[53] D. Kapec, A.-M. Raclariu, and A. Strominger, Area, entanglement entropy and supertranslations at null infinity, Classical Quantum Gravity **34,** 165007 (2017).

[54] K. Narayan, Extremal surfaces in de Sitter spacetime, Phys. Rev. D **91,** 126011 (2015).

[55] Y. Sato, Comments on entanglement entropy in the dS/CFT correspondence, Phys. Rev. D **91,** 086009 (2015).

[56] C. Holzhey, F. Larsen, and F. Wilczek, Geometric and renormalized entropy in conformal field theory, Nucl. Phys. **B424,** 443 (1994).

[57] P. Calabrese and J. L. Cardy, Entanglement entropy and quantum field theory, J. Stat. Mech. (2004) P06002.

[58] L.-Y. Hung, R. C. Myers, and M. Smolkin, On holographic entanglement entropy and higher curvature gravity, J. High Energy Phys. 04 (2011) 025.

[59] G. Barnich and C. Troessaert, Symmetries of Asymptotically Flat 4 Dimensional Spacetimes at Null Infinity Revisited, Phys. Rev. Lett. **105,** 111103 (2010).

[60] G. Barnich and C. Troessaert, Supertranslations call for superrotations, *Proc. Sci.*, CNCFG2010 (2010) 010 [arXiv:1102.4632].

[61] S. Pasterski and H. Verlinde, Chaos in celestial CFT, J. High Energy Phys. 08 (2022) 106.

[62] I. S. Gradshteyn and I. M. Ryzhik, *Table of Integrals, Series, and Products* (Elsevier/Academic Press, Amsterdam, 2007).